Causal Control of the Thalamic Reticular Nucleus Using Optogenetic And Novel Chemogenetic Approaches

By

Bryan T. Higashikubo

B.S. Psychology
Duke University, 2004

SUBMITTED TO THE DEPARTMENT OF BRAIN AND COGNITIVE SCIENCES IN PARTIAL FULFILLMENT OF THE REQUIREMENTS FOR THE DEGREE OF

DOCTOR OF PHILOSOPHY IN NEUROSCIENCE
AT THE
MASSACHUSETTS INSTITUTE OF TECHNOLOGY

JUNE 2016 [September 2016]

Signature of Author: Signature redacted
Department of Brain and Cognitive Sciences
June 1, 2016

Certified by: Signature redacted
Christopher I. Moore
Associate Professor of Neuroscience
Thesis Supervisor

Accepted by: Signature redacted
Matthew A. Wilson
Sherman Fairchild Professor of Neuroscience and Picower Scholar
Director of Graduate Education for Brain and Cognitive Sciences

Abstract

Incoming sensory information from all modalities, with the exception of olfaction, synapses in the thalamus on the way to neocortex. This sensory relay is uniquely positioned to act as a gate, to determine which inputs from the periphery are processed by the neocortex. A key 'guardian' of the gate may be the thalamic reticular nucleus (TRN). The TRN is a primary source of GABAergic input to thalamic relay nuclei. The TRN projects directly to the rest of thalamus, generating feedforward and feedback inhibition. It is therefore positioned to mediate forebrain function, and specifically the computations of the neocortex-thalamic loop. Accordingly, failures of the normal dynamics of the TRN are prominent in disease

Thalamocortical and corticothalamic projections synapse within this nucleus, and it is subject to a variety of neuromodulatory influences. Depolarization of TRN neurons, and their subsequent firing, is driven by a variety of sources on a range of time scales. The TRN receives excitatory inputs ranging from single spikes to sustained tonic firing to bursting in thalamic relay neurons or layer 6 of neocortex. The temporal dynamics of these inputs, and their spatial organization, can drive different types of firing behavior in TRN. Layer 6 cells form strong synapses in the TRN and even sparse activity in this layer would be predicted to drive substantial inhibition *in vivo*. Primary thalamocortical relay projections branch into the TRN on their way to sensory cortices, and the nature of this excitatory input reflects the functional modes of the relay nuclei. Inputs include tonic firing that reflects high fidelity to peripheral input, as well as extended bouts of bursting, similar to that seen in TRN itself. In sum, a variety of inputs can excite TRN neurons on different time scales. Understanding how these different patterns may regulate excitability in general, and burst activity specifically, is key to understanding thalamocortical function.

The Moore laboratory previously showed that TRN activation could modulate firing and bursting in relay neurons, and induce spindles in the neocortex. In these experiments, the activity of TRN cells during stimulation could only be inferred from downstream effects on spiking and spindle rhythms. Characterizing responses within TRN using a similar stimulation protocol provided a more complete view of the circuit activity underlying this evoked behavior.

In Chapter 2 I provided optogenetic input while characterizing multi-unit responses in the TRN and well-sorted single units. I found that longer duration activation drove enhanced bursting and decreased latency to bursting. I also discovered two new types of cell responses, a more sensitive 'non-linear' cell type that was prone to sustained responses and to bursting, and a more 'linearly' responsive cell class that fired in direct proportion to the duration of stimulation. These findings provide direct predictions as to the behavior of TRN neurons in response to a range of natural depolarizing inputs, and a guide for the optical control of this key structure in studies of network function and behavior.

As indicated by the availability of neuromodulatory inputs to TRN, and its apparent role in basic state changes such as sleep and wakefulness, long-term shifts in its depolarization are also likely essential to normal brain function. Optogenetics has rapidly become a standard technique in systems neuroscience, and its genetic specificity and rapid development of

new compounds has revolutionized our ability to causally manipulate neural circuits. While the use of light to drive cellular reactions brings a number of advantages when compared to electrical stimulation, there are still many limitations, especially *in vivo*. Light delivery through tissue is problematic in the intact brain, so targeting deep structures relies on implanted fiber optics and/or LEDs. These methods are not ideal for illuminating large or irregularly-shaped regions without using high light intensity or large arrays of invasive devices. I have been key in inventing a new approach using bioluminescent light to drive optogenetic responses ('BL-OG'). This approach leverages the variety of light sensitive molecules and bioluminescent emitters while providing a means of chemical control. BL-OG combines the cell-type specificity of conventional optogenetics with the potential for non-invasive, system-wide activation. In Chapter 3, I review both this new method and some of my contributions to its realization, specifically demonstrating its functionality in the TRN *in vitro* and *in vivo*.

Thesis Supervisor: Christopher I. Moore

Acknowledgements

I would like to thank the members of the Moore lab, past and present, with whom I worked at first as a technician and then as a graduate student. First, I want to acknowledge my advisor, Chris Moore, who I've worked with for the last ~10 years. Chris has been a great mentor, and even with many changes of personnel, the lab reflects his collaborative nature and wide range of intellectual interests. My whole academic path owes a lot to Chris taking a chance on hiring me as a tech—I sent him an email while looking for interesting neurophysiology labs and it turned into an exciting job and then a PhD.

My first work in the lab was done with Mark Andermann, who showed me the proverbial ropes and taught me techniques that I use to this day. Jason Ritt and Dominique Pritchett were there when I got started, and were great sources of insight as well as good people to have around if you're doing late-night science at the MBL. Ulf Knoblich, Chris Deister, and Tyler Brown were people who I learned a lot from, both scientifically and culturally—they helped to ensure that the Moore lab was the place to be for neuroscience discussions as well as solid recommendations for music and/or food. I spent a lot of time in dark rooms with Ethan Skowronski-Lutz and Rosa Cao while doing imaging, and I later shared a rig with Katy Thorn, all of which worked out incredibly well even when things needed to be fixed. I'd also like to thank Jakob Voigts and Nathan Vierling-Claassen, for their help building stuff, debugging stuff, and conversations on the long commute. Finally, no mention of the Moore lab would be complete without thanking the lab managers who kept everything going. In my tenure with the lab, Cheryl Cheney, Alexis Bradshaw, Qian Wan, Cassie Burley, Kia Salehi, and Emma Lehmann have all been essential for anything to get done.

I'd next like to specifically thank collaborators and people whose work directly influenced my thesis. For chapter 2, a key inspiration for my experiments was work done previously in lab by Mike Halassa and Josh Siegle. For chapter 3, a number of people were essential for the whole project. Ute Hochgeschwender and her group were responsible for designing the luminopsin constructs that I used and also provided huge amounts of guidance and preliminary data. Initial testing of LMO3 in slice was made possible by the help of Shane Crandall and the lab of Barry Connors. Liz McDonnell was a collaborator for both in vivo and in vitro work.

A special thanks to the administrative staff for the BCS graduate program, who were knowledgeable advocates for us students, even if we were at different universities and forgot to check our email sometimes.

I have to thank my family, who has supported me throughout my whole graduate career. My parents provided love, support, and a desire for knowledge that brought me to where I am today. My brother is a great friend who can now truly understand the ups and downs of grad school.

Finally, I'd like to thank Katie Wu, who supported me through random work hours, frantic thesis writing, and general PhD madness. I love you and couldn't have done it without you.

Table of Contents

Chapter 1

Introduction

Overview

My primary research interests are in the neural circuit mechanisms that underlie sensory perception—given the massive amount of data taken in from a constantly changing outside world, the brain is capable of forming a seemingly cohesive representation of our physical reality that highlights behaviorally relevant information.

My thesis research approached these questions at the level of the thalamus, which is central to the flow of sensory signals to cortex and is profoundly important in the regulation of brain state. My interest in the thalamic reticular nucleus is tied to its position within the thalamocortical pathway and its particular importance in the rodent somatosensory system, the primary model used in the Moore lab. The use of optogenetics in TRN by Halassa and Siegle (Halassa et al., 2011) showed the utility of the technique for targeting such a small subcortical structure in the mouse, and my first project was to characterize the response properties of TRN cells through multielectrode recording and optical stimulation. In addition to general parameterization of optogenetics in this population, I found evidence for functional heterogeneity within TRN that became apparent with modulation of stimulus duration. My subsequent work used these data as a baseline for investigating a novel technique for brain stimulation that is particularly relevant for clinical and research use in the thalamus.

TRN and sensory gating

Incoming sensory information from all modalities, with the exception of olfaction, synapses in the thalamus on the way to neocortex (Pinault, 2004). This sensory relay is uniquely positioned to act as a gate, to determine which inputs from the periphery are processed by the neocortex (Crick, 1984). A gating mechanism has been hypothesized to underlie attentional processes, which are often conceived as a 'spotlight' that selects behaviorally relevant information through a spatially delimited/topographic enhancement or suppression of information. While effects of attention on behavior are well characterized, and much has been studied about attentional modulation of cortical activity (ie V4 in the monkey) (Desimone and Duncan, 1995; Reynolds and Chelazzi, 1999; Treue and Maunsell, 1999), less is known about its role earlier in sensory processing. Inhibitory circuits provide a way for the thalamus to act as more than a passive relay that routes peripheral signals to the appropriate higher areas—it could be used to filter out irrelevant information before it competes for resources further along the pathway.

A primary source of GABAergic input to thalamic relay nuclei that send information to neocortex is the thalamic reticular nucleus (TRN), a thin shell of neurons enveloping the thalamus (Jones, 1975). Projections from thalamocortical and corticothalamic cells synapse within this nucleus, and the TRN projects directly to the rest of thalamus, generating feedforward and feedback inhibition in this structure. This source of inhibition is particularly important in rodents, which lack local inhibitory interneurons in somatosensory thalamus and many other nuclei.

These properties of the TRN led Francis Crick to postulate that it may be key to the attentional spotlight, stating that the TRN might be described as the "guardian of the gateway" (Crick, 1984). Recent monkey neurophysiological studies support this idea, showing that TRN activity in the representation where selective attention is allocated are modulated in cross-modal and within-modality tasks (McAlonan et al., 2000; McAlonan and Brown, 2002; McAlonan et al., 2006; 2008). Under this framework, the TRN could exert an influence on attention at very early levels of primary sensory pathways, as topographically specific inhibition of relay nuclei is a potent mechanism for blocking inattended stimuli before even reaching the cortex. Studies in the rodent somatosensory thalamus have shown the appropriate anatomical substrate for this level of spatial control, as well as patterns of interconnection that could allow for complex lateral interaction (Bourassa et al., 1995; Pinault et al., 1995; Deschênes et al., 1996; Pinault and Deschênes, 1998a; 1998b; Desîlets-Roy et al., 2002). The degree of innervation in TRN from both TC and CT fibers positions the nucleus to respond to feedback from primary sensory cortices, while input from the prefrontal cortex (as observed in monkeys) (Zikopoulos and Barbas, 2006)could provide top-down control of the attentional spotlight, as determined by behavioral state and cognitive demand.

TRN and rhythmicity

A well-known property of thalamic projection neurons is their ability to fire action potentials in different modes, tonic or bursting, depending on the state of the network. A burst consists of multiple spikes fired in rapid succession (e.g., with an interval <4ms) preceded by periods of quiescence >100ms (Swadlow and Gusev, 2001). "Bursting" is a

widely applied descriptor of neural activity, but in thalamic nuclei, this term specifically refers to a period of high frequency action potential firing mediated by a large underlying calcium event (a calcium "spike") (Crunelli et al., 1989; Huguenard and Prince, 1992; Coulon et al., 2009). In vitro studies have shown that many thalamic neurons (including thalamocortical projection cells and TRN cells) express T-type calcium channels that cause calcium spikes and bursts after a period of hyperpolarization. The TRN inhibits thalamocortical neurons, causing a hyperpolarization that de-inactivates T-channels. Upon release of inhibition, these channels are available to open, leading to a calcium spike with a burst of multiple concurrent sodium action potentials. The activity of these relay cells in turn provides an excitatory input to the TRN, forming an oscillatory loop.

The change from tonic to burst firing denotes a shift in thalamic network dynamics, but the role of bursting in information processing is debated. Some studies have argued that a burst is highly efficient at relaying information by virtue of the postsynaptic impact of several spikes fired in short succession (Swadlow and Gusev, 2001). In a contrasting view (Llinás and Steriade, 2006), bursting represents a state of inattention and impoverished signal relay. In support of this view, recent studies have shown that alpha rhythms—widely believed to emerge from thalamic bursting at 5-15 Hz—occur in specific parts of sensory maps that are disattended during task performance (Worden et al., 2000; Banerjee et al., 2011; Foxe and Snyder, 2011). In either case—whether bursting is an optimal signal relay or the signature of a decreased probability of information relay—understanding any differences in the relative expression these events across thalamic nuclei will provide useful insight for leading theories of thalamocortical dynamics.

As stated previously, the rapid firing of multiple action potentials in a burst can be highly effective for driving activity in post-synaptic targets, potentially enhancing signal relay in the brain (Lesica, 2004; Alitto and Usrey, 2005; Lesica et al., 2006; Stanley, 2013). Excessive expression of this powerful activity pattern in thalamus is hypothesized to be causal in several diseases (Llinás et al., 1999). As a cardinal example, multiple types of epileptic seizures are believed to be driven by hyper-synchronized rhythmic bursting in the thalamic reticular nucleus (TRN) and in thalamic relay neurons that project to the neocortex (Beenhakker and Huguenard, 2009). The TRN is a shell of inhibitory neurons that target and hyperpolarize thalamic relay cells, generating rebound bursts. Epileptic seizures emerging from neocortical injury, and absence seizures, the most common form in children, are both believed to emerge from overly robust rates and synchrony of thalamic bursting (Avanzini et al., 1996; Beenhakker and Huguenard, 2009; Paz et al., 2013). Thalamic burst-driven seizure activity is hypothesized to be an altered form of endogenous patterns observed in slow-wave sleep called spindles, bouts of rhythmic thalamic bursting typically lasting ~.5-1.5 seconds (Kostopoulos, 2000; Beenhakker and Huguenard, 2009).

Chapter 2: Background and Motivation

The depolarization of TRN neurons, and their subsequent firing, is driven by a variety of sources on a range of time scales. The TRN receives excitatory inputs ranging from single spikes to sustained tonic firing to bursting in thalamic relay neurons or layer 6 of neocortex(de Curtis et al., 1989; Contreras et al., 1992; Bourassa et al., 1995; Avanzini et al., 1996; Sherman and Guillery, 1996; Pinault and Deschênes, 1998a; Jones, 2004; Crandall et

al., 2015). The temporal dynamics of these inputs, as well as their spatial organization, can drive different types of firing behavior in TRN(Lam and Sherman, 2010; 2011). Layer 6 cells form strong synapses in the TRN(Lam and Sherman, 2010; Crandall et al., 2015), and even sparse activity in this layer would be predicted to engage substantial inhibition *in vivo*. Primary thalamocortical relay projections branch into the TRN on their way to sensory cortices, and the nature of this excitatory input reflects the functional modes of the relay nuclei. Inputs include tonic firing that reflects high fidelity to peripheral input, as well as extended bouts of bursting, similar to that seen in TRN itself. In sum, a variety of inputs can excite TRN neurons on different time scales. Understanding how these different patterns may regulate excitability in general, and burst activity specifically, is key to understanding thalamocortical relay and function. In addition to the basic science questions associated with this variability, characterization of optogenetic responses in TRN is vital for future experimental planning. The TRN is an appealing target for research into sensory perception and neurological disease, and understanding how different modes of stimulation affect its activity is crucial to interpreting its role in these broader contexts.

In our lab, we previously showed that putative TRN activation could modulate firing and bursting in relay neurons, and induce spindles in the neocortex (Halassa et al., 2011). In these experiments, stimulation was confined to the TRN using implanted optical fibers in the VGAT-ChR2 mouse, but electrophysiological recordings were targeted to the somatosensory relay thalamus and the cortex. As a result, the activity of TRN cells during stimulation could only be inferred from downstream effects on spiking and spindle rhythms. Characterizing the responses within TRN using a similar stimulation protocol

provided a more complete view of the circuit activity underlying evoked burst and spindle behavior.

As such, my work in Chapter 2 was important at several levels. I provided optogenetic input while characterizing multi-unit responses in the TRN and well-sorted single units. As reviewed below, I found that longer duration activation drove enhanced bursting and decreased latency to bursting. I also discovered two new types of cell responses, a more sensitive 'non-linear' cell type that was prone to sustained responses and to bursting, and a more 'linearly' responsive cell class that fired in direct proportion to the duration of stimulation. These findings provide direct predictions as to the behavior of TRN neurons in response to a range of natural depolarizing inputs, and a guide for the optical control of this key structure in studies of network function and behavior.

Chapter 3: Next Step Methods for Long Time Scale TRN Regulation—Bioluminescent Optogenetics

The TRN is believed to be crucial to the regulation of long time scale state transitions, e.g., between sleep and wakefulness. As such, developing methods for minimally-invasive control of this structure on such time scales has high utility to my research goals. Optogenetics has rapidly become a standard technique in systems neuroscience, and its genetic specificity and rapid development of new compounds has revolutionized our ability to causally manipulate neural circuits. While the use of light to drive cellular reactions brings a number of advantages when compared to electrical stimulation, there are still many limitations to this approach, especially when applied *in vivo*. Light delivery through

tissue is problematic in the intact brain, so targeting deep structures relies on implanted fiber optics and/or LEDs. These methods are not ideal for illuminating large or irregularly-shaped regions without using high light intensity or large arrays of invasive devices. I have been key in inventing a new methodological approach using bioluminescent light to drive optogenetic responses ('BL-OG'; (Berglund et al., 2013; Tung et al., 2015; Berglund et al., 2016a; 2016b)). This approach leverages the revolution in new light sensitive molecules, and the wide array of bioluminescent options, while providing a means of chemiluminescent control. BL-OG combines the cell-type specificity of conventional optogenetics with the potential for non-invasive, system-wide activation of opsins. In Chapter 3, I review both the new method and some of my contributions to its realization.

References

Alitto HJ, Usrey WM. Dynamic properties of thalamic neurons for vision. *Prog Brain Res* 149: 83–90, 2005.

Avanzini G, de Curtis M, Franceschetti S, Sancini G, Spreafico R. Cortical versus thalamic mechanisms underlying spike and wave discharges in GAERS. *Epilepsy Res* 26: 37–44, 1996.

Banerjee S, Snyder AC, Molholm S, Foxe JJ. Oscillatory alpha-band mechanisms and the deployment of spatial attention to anticipated auditory and visual target locations: supramodal or sensory-specific control mechanisms? *J Neurosci* 31: 9923–9932, 2011.

Beenhakker MP, Huguenard JR. Neurons that fire together also conspire together: is normal sleep circuitry hijacked to generate epilepsy? *Neuron* 62: 612–632, 2009.

Berglund K, Birkner E, Augustine GJ, Hochgeschwender U. Light-emitting channelrhodopsins for combined optogenetic and chemical-genetic control of neurons. *PLoS ONE* 8: e59759, 2013.

Berglund K, Clissold K, Li HE, Wen L, Park SY, Gleixner J, Klein ME, Lu D, Barter JW, Rossi MA, Augustine GJ, Yin HH, Hochgeschwender U. Luminopsins integrate opto- and chemogenetics by using physical and biological light sources for opsin activation. *Proceedings of the National Academy of Sciences* 113: E358–67, 2016a.

Berglund K, Tung JK, Higashikubo B, Gross RE, Moore CI, Hochgeschwender U. Combined Optogenetic and Chemogenetic Control of Neurons. *Methods Mol Biol* 1408: 207–225, 2016b.

Bourassa J, Pinault D, Deschênes M. Corticothalamic projections from the cortical barrel field to the somatosensory thalamus in rats: a single-fibre study using biocytin as an anterograde tracer. *Eur J Neurosci* 7: 19–30, 1995.

Contreras D, Dossi RC, Steriade M. Bursting and tonic discharges in two classes of reticular thalamic neurons. *J Neurophysiol* 68: 973–977, 1992.

Coulon P, Herr D, Kanyshkova T, Meuth P, Budde T, Pape H-C. Burst discharges in neurons of the thalamic reticular nucleus are shaped by calcium-induced calcium release. *Cell Calcium* 46: 333–346, 2009.

Crandall SR, Cruikshank SJ, Connors BW. A corticothalamic switch: controlling the thalamus with dynamic synapses. *Neuron* 86: 768–782, 2015.

Crick F. Function of the thalamic reticular complex: the searchlight hypothesis. *Proc Natl Acad Sci USA* 81: 4586–4590, 1984.

Crunelli V, Lightowler S, Pollard CE. A T-type Ca2+ current underlies low-threshold Ca2+ potentials in cells of the cat and rat lateral geniculate nucleus. *J Physiol (Lond)* 413: 543–

561, 1989.

de Curtis M, Spreafico R, Avanzini G. Excitatory amino acids mediate responses elicited in vitro by stimulation of cortical afferents to reticularis thalami neurons of the rat. *Neuroscience* 33: 275–283, 1989.

Deschênes M, BOURASSA J, Doan VD, Parent A. A single-cell study of the axonal projections arising from the posterior intralaminar thalamic nuclei in the rat. *Eur J Neurosci* 8: 329–343, 1996.

Desimone R, Duncan J. Neural mechanisms of selective visual attention. *Annu Rev Neurosci* 18: 193–222, 1995.

Desîlets-Roy B, Varga C, Lavallée P, Deschênes M. Substrate for cross-talk inhibition between thalamic barreloids. *J Neurosci* 22: RC218, 2002.

Foxe JJ, Snyder AC. The Role of Alpha-Band Brain Oscillations as a Sensory Suppression Mechanism during Selective Attention. *Front Psychol* 2: 154, 2011.

Halassa MM, Siegle JH, Ritt JT, Ting JT, Feng G, Moore CI. Selective optical drive of thalamic reticular nucleus generates thalamic bursts and cortical spindles. *Nat Neurosci* (July 24, 2011). doi: 10.1038/nn.2880.

Huguenard JR, Prince DA. A novel T-type current underlies prolonged Ca(2+)-dependent burst firing in GABAergic neurons of rat thalamic reticular nucleus. *Journal of Neuroscience* 12: 3804–3817, 1992.

Jones E. Some aspects of the organization of the thalamic reticular complex. *J Comp Neurol.*

Jones EG. Some aspects of the organization of the thalamic reticular complex. *J Comp Neurol* 162: 285–308, 2004.

Kostopoulos GK. Spike-and-wave discharges of absence seizures as a transformation of sleep spindles: the continuing development of a hypothesis. *Clin Neurophysiol* 111 Suppl 2: S27–38, 2000.

Lam Y-W, Sherman SM. Functional organization of the somatosensory cortical layer 6 feedback to the thalamus. *Cereb Cortex* 20: 13–24, 2010.

Lam Y-W, Sherman SM. Functional organization of the thalamic input to the thalamic reticular nucleus. *J Neurosci* 31: 6791–6799, 2011.

Lesica NA, Weng C, Jin J, Yeh C-I, Alonso J-M, Stanley GB. Dynamic Encoding of Natural Luminance Sequences by LGN Bursts. *PLoS Biol* 4: e209, 2006.

Lesica NA. Encoding of Natural Scene Movies by Tonic and Burst Spikes in the Lateral Geniculate Nucleus. *J Neurosci* 24: 10731–10740, 2004.

Llinás RR, Ribary U, Jeanmonod D, Kronberg E, Mitra PP. Thalamocortical dysrhythmia: A neurological and neuropsychiatric syndrome characterized by magnetoencephalography. *Proc Natl Acad Sci USA* 96: 15222–15227, 1999.

Llinás RR, Steriade M. Bursting of thalamic neurons and states of vigilance. *J Neurophysiol* 95: 3297–3308, 2006.

McAlonan K, Brown VJ, Bowman EM. Thalamic reticular nucleus activation reflects attentional gating during classical conditioning. *J Neurosci* 20: 8897–8901, 2000.

McAlonan K, Brown VJ. The thalamic reticular nucleus: more than a sensory nucleus? *Neuroscientist* 8: 302–305, 2002.

McAlonan K, Cavanaugh J, Wurtz RH. Attentional modulation of thalamic reticular neurons. *J Neurosci* 26: 4444–4450, 2006.

McAlonan K, Cavanaugh J, Wurtz RH. Guarding the gateway to cortex with attention in visual thalamus. *Nature* 456: 391–394, 2008.

Paz JT, Davidson TJ, Frechette ES, Delord B, Parada I, Peng K, Deisseroth K, Huguenard JR. Closed-loop optogenetic control of thalamus as a tool for interrupting seizures after cortical injury. *Nat Neurosci* 16: 64–70, 2013.

Pinault D, Bourassa J, Deschênes M. The Axonal Arborization of Single Thalamic Reticular Neurons in the Somatosensory Thalamus of the Rat. *European Journal of Neuroscience* 7: 31–40, 1995.

Pinault D, Deschênes M. Anatomical evidence for a mechanism of lateral inhibition in the rat thalamus. *Eur J Neurosci* 10: 3462–3469, 1998a.

Pinault D, Deschênes M. Projection and innervation patterns of individual thalamic reticular axons in the thalamus of the adult rat: a three-dimensional, graphic, and morphometric analysis. *J Comp Neurol* 391: 180–203, 1998b.

Pinault D. The thalamic reticular nucleus: structure, function and concept. *Brain Research Reviews* 46: 1–31, 2004.

Reynolds JN, Chelazzi L. Competitive mechanisms subserve attention in macaque areas V2 and V4. *Journal of Neuroscience*.

Sherman SM, Guillery RW. Functional organization of thalamocortical relays. *J Neurophysiol* 76: 1367–1395, 1996.

Stanley GB. Reading and writing the neural code. *Nat Neurosci* 16: 259–263, 2013.

Swadlow HA, Gusev AG. The impact of "bursting" thalamic impulses at a neocortical synapse. *Nat Neurosci* 4: 402–408, 2001.

Treue S, Maunsell JHR. Effects of attention on the processing of motion in macaque middle temporal and medial superior temporal visual cortical areas. *J Neurosci* 19: 7591–7602, 1999.

Tung JK, Gutekunst C-A, Gross RE. Inhibitory luminopsins: genetically-encoded bioluminescent opsins for versatile, scalable, and hardware-independent optogenetic inhibition. *Sci Rep* 5: 14366, 2015.

Worden MS, Foxe JJ, Wang N, Simpson GV. Anticipatory biasing of visuospatial attention indexed by retinotopically specific alpha-band electroencephalography increases over occipital cortex. *J Neurosci* 20: RC63, 2000.

Zikopoulos B, Barbas H. Prefrontal projections to the thalamic reticular nucleus form a unique circuit for attentional mechanisms. *J Neurosci* 26: 7348–7361, 2006.

Chapter 2

Systematic Examination of the Impact of Depolarization Duration on Thalamic Reticular Nucleus Firing *in vivo*

Author contributions:
BTH and CIM designed experiments, BTH collected and analyzed data, BTH and CIM drafted and edited the manuscript and approved the final version.

A version of this chapter is under review as:

Systematic Examination of the Impact of Depolarization Duration on Thalamic Reticular Nucleus Firing *in vivo*

Bryan Higashikubo and Christopher I. Moore

Abstract:
The thalamic reticular nucleus (TRN) is optimally positioned to regulate information processing and state dynamics in dorsal thalamus. Distinct inputs depolarize TRN on a variety of time scales, including thalamocortical afferents, corticothalamic 'feedback', and neuromodulatory influences. Here, we systematically tested the immediate and sustained effects of depolarization duration on TRN firing *in vivo* using selective optogenetic drive. In VGAT-ChR2 mice, well-isolated TRN single units (SU: N=100 neurons) responded at brief latency (≤5 milliseconds) to optical pulses. These units, and multi-unit activity (MUA) on corresponding electrodes, were analyzed in detail. Burst-like events occurred after light cessation in 74% of MUA sites, and 16% of SU. Increasing optical duration from 2 to 330 milliseconds enhanced burst probability, and decreased the latency to the first burst after stimulation. All neurons demonstrated a 'plateau' firing response lasting 20–30 milliseconds in response to light, but significant heterogeneity existed in the minimal stimuli required to drive this response. Two distinct types were evident, more sensitive 'non-linear' neurons that were already driven to the plateau response by 2 or 5 millisecond light pulses, versus 'linear' neurons that fired in proportion to optical duration, and reached the plateau with ~20 millisecond optical drive. Non-linear neurons showed higher evoked firing rates and burst probability, but spontaneous rate did not differ between types. These findings provide direct predictions as to TRN responses to a range of natural depolarizing inputs, and a guide for the optical control of this key structure in studies of network function and behavior.

New and Noteworthy: The thalamic reticular nucleus receives depolarizing inputs on a wide range of timescales. Excitatory optogenetic stimuli of different durations were given

to the TRN *in vivo* and cell activity was monitored during and after stimulation. Longer periods of stimulation were associated with increased post-stimulus activity. Direct responses to stimuli revealed two categories: units with a response duration matched to stimulus duration and units that showed nonlinear behavior.

Introduction

Thalamic reticular nucleus (TRN) neurons play a key role in thalamocortical dynamics. The TRN makes GABAergic projections to first and higher-order thalamic nuclei, providing a major source of hyperpolarization to relay cells (Pinault, 2004). The TRN is therefore positioned to regulate the flow of signals between the periphery and neocortex, potentially gating information during active processing (Crick, 1984; Weese et al., 1999; Yu et al., 2009). Primate and mouse studies have shown modulation of TRN with allocation of selective attention (McAlonan et al., 2000; McAlonan and Brown, 2002; McAlonan et al., 2006; Wimmer et al., 2015), and TRN receives connections from brain regions involved in decision making, such as the prefrontal cortex, that could direct its activity based on behavioral context (Zikopoulos and Barbas, 2006). The TRN is also widely implicated in regulating dorsal thalamic and neocortical dynamics during less active states including in sleep (Steriade, 1985; Steriade and Llinas, 1988; Steriade et al., 1993; Huguenard and McCormick, 2007).

The duration and firing pattern of TRN neurons are likely both key determinants in controlling its downstream partners. Both TRN and thalamic relay neurons express T-type low threshold calcium channels that cause bursting following hyperpolarization (Crunelli et al., 1989; Huguenard and Prince, 1992). Inhibition generated by TRN, particularly the robust hyperpolarization generated by TRN burst firing, can drive rebound bursting in relay cells that feed back to TRN (Bal and McCormick, 1993; Bal et al., 1995). This loop is believed important in establishing sustained rhythmic activity, including repeated bursting in events such as spindles (Steriade et al., 1985).

Changes in factors that regulate excitatory dynamics in TRN cells are also key to brain health. Abnormalities in TRN firing and sleep spindles are observed in schizophrenia (Austin et al., 2004; Ferrarelli et al., 2007; 2010; Pinault, 2011; Pratt and Morris, 2015), and a mutation of the CAv 3.3 T-type channels expressed in TRN alters TRN firing patterns and predicts schizophrenic phenotype (Liu et al., 2011; Astori et al., 2011; Schizophrenia Working Group of the Psychiatric Genomics Consortium, 2014). Altered patterns of TRN firing are also implicated in absence epilepsy, where seizures are associated with spike-wave discharges driven by thalamic bursting (Pinault et al., 1998; Llinás et al., 1999; Slaght et al., 2002; Crunelli et al., 2011; Tringham et al., 2012; Paz et al., 2013).

Depolarization of TRN neurons, and their subsequent firing, is driven by a variety of sources on a variety of time scales. The TRN receives synaptic input from both thalamocortical and corticothalamic axons that pass through its extent. While relatively few studies have recorded from identified corticothalamic cells, these layer 6 neurons fire are known to fire in a highly sparse manner, with low spontaneous and sensory-evoked firing rates, and a low probability of firing to sensory stimuli (< 10% of identified neurons), even in topographically aligned positions in primary sensory neocortex (Temereanca and Simons, 2004; Kwegyir-Afful and Simons, 2009). However, brief activity in the layer 6 input to TRN is particularly effective in driving depolarization. Large excitatory post-synaptic potentials with rapid rise times are observed in TRN neurons after single spikes or brief activation of corticothalamic cells (Golshani et al., 2001; Crandall et al., 2015).

Correspondingly, brief corticothalamic input also generates robust suppression in relay neurons (Landisman and Connors, 2007; Mease et al. 2014).

Primary thalamocortical relay neurons show activity on a wide variety of time scales, firing single spikes, sustained trains of single action potentials and bursts in response to sensory drive, and revealing a range of patterns of afferent adaptation (Diamond et al., 1992; Castro-Alamancos and Connors, 1996; Castro-Alamancos, 2002; Rigas and Castro-Alamancos, 2007; Lam and Sherman, 2011). Relay thalamic inputs to the TRN can, in concept, provide a variety of time scales of depolarization dependent on state and context.

In addition to the single spikes or epochs of bursting provided by cortical and thalamic inputs, the TRN receives modulatory inputs from a number of different brain structures. Cholinergic projections to the TRN have multiple origins, including projections from the brainstem that are associated with arousal (Boucetta et al., 2014) as well as a basal forebrain projection that can act on a synaptic timescale to drive firing followed by desychronization (Pita-Almenar et al., 2014). In addition to connections between individual inhibitory cells within the TRN, the nucleus also receives inhibitory inputs from the basal ganglia, with projections from the substantia nigra pars reticulata (SNr) and the globus pallidus (Gandia et al., 1993) that could be a substrate for disinhibition of reticular targets or for burst regulation. The neuropeptide somatostatin is expressed throughout the TRN (Graybiel et al. 1983), and has been shown to influence oscillatory activity in slice preparations (Sun et al., 2002).

In sum, a variety of inputs can excite TRN neurons on different time scales. Understanding how these different patterns may regulate excitability in general, and burst activity specifically, is key to understanding thalamocortical relay and function.

In addition to diversity in types of depolarization the TRN may receive, TRN cells themselves exhibit functional and anatomical heterogeneity (Lee et al., 2007; Halassa et al., 2014; Lee et al., 2014; Kimura and Imbe, 2015). Axonal arborization of TRN neurons projecting to first- and higher-order thalamic nuclei in the same sensory modality varies by target (Cox et al., 1996). In rodent somatosensory thalamus, projections to VPM are well defined and correspond to individual barreloids, while projections to POm are more diffuse(Pinault and Deschênes, 1998b; 1998a; Desîlets-Roy et al., 2002). Within the TRN, somata of cells targeting different regions are biased to occur in distinct tiers(Clemence and Mitrofanis, 1992; Pinault and Deschênes, 1998a; 1998b; Desîlets-Roy et al., 2002).

At a functional level, Contreras et al. (Contreras et al., 1992) described two types of cells in the reticular nucleus of the anesthetized cat, type I cells that exhibit standard T-current mediated bursting, and type II cells that did not burst and showed less adaptation when driven at high frequencies. Recent work from Halassa et al. (Halassa et al., 2014) also found evidence for functional distinction between two types of TRN cells in mice. In that study, firing rates were either negatively or positively correlated with spindle and delta oscillation expression. Cells negatively correlated with spindles were more active during higher arousal states, suggesting a more tonic firing mode for this class.

To understand the potential role of this key node in controlling thalamocortical dynamics, and the potential for heterogeneity in response types in response to diverse inputs, we studied TRN cell responses to changes in stimulus duration in an intact, *in vivo* network. A powerful tool for manipulation of an identified cell population is optogenetics. Consistent with the hypothesized role of TRN cells, direct optogenetic drive of this structure causes bursting in relay neurons and sleep spindles *in vivo* (Halassa et al., 2011). While showing that bursting can result from TRN activation, this prior study did not assess the impact of optogenetic drive on TRN neurons themselves, nor did it seek to systematically understand the impact of the duration of stimulation on network dynamics.

To directly address these questions, we used an acute preparation to study TRN units activated at short latencies after light onset (i.e., those cells presumably expressing ChR2). Here we report that bursting probability in TRN neurons depends systematically on, and varies positively with, the duration of stimulation. We further discovered two classes of TRN neurons by their responses to direct optical activation. One group showed greater sensitivity to brief light pulses, including a greater propensity to bursting, but also showed greater response saturation with increasing stimulus duration. In contrast, the second cell type showed a near linear increase in firing with increased stimulus duration, but a lower propensity to bursting. These findings provide direct predictions as to the behavior of TRN neurons in response to a range of natural depolarizing inputs, and a guide for the optical control of this key structure in studies of network function and behavior.

Materials and Methods

Optrode construction

Prefabricated 16-channel linear electrode arrays (Neuronexus technology, A1x16-5mm-25-177, with 25 μm spacing between 177 μm^2 contacts) were chosen as the basis for thalamic optrodes. Multimode optical fiber cannulae (105μm core diameter, coating stripped, Thorlabs) were positioned using a surgical microscope to rest ~200μm above the top electrode contact of the array without touching the probe shank, and fixed in place with a silicone elastomer. The back end of each fiber was terminated in a 1.25mm ceramic ferrule that was anchored to the probe PCB by a 3D printed bracket (**Fig 1A** schematic, **Fig** 1B side view showing fiber orientation). This configuration provided a stable attachment point for an optical patch cable and strain relief for the fiber during connection and disconnection. Designs are available at Open Ephys (www.open-ephys.org).

Animal preparation and electrophysiology

All recordings were performed in lightly anesthetized (0.75 - 1.1% isoflurane) adult VGAT-ChR2 mice (2-4 weeks old) fixed in a stereotaxic frame with an integrated nosecone. A craniotomy was made at approximate coordinates 1.9mm lateral and 1.7mm posterior to bregma, and custom optrodes were lowered to ~3mm below the cortical surface. Simultaneous laser stimulation and recordings were conducted during electrode penetration to confirm the localization of probe contacts to the TRN, as indicated by short latency optical spiking responses and thin action potential wave forms. Recordings were

obtained with the Neuralynx Cheetah data acquisition system, with 16 amplified electrode channels sampled at 30.3kHz and additional analog inputs used to register the timing of stimulus delivery.

Optical stimulus delivery

Light pulses were delivered from a 100mW, 472nm DPSS laser coupled to a multimode patch cable. Stimulus intensity was measured as 7-8mW at the end of the optrode. Stimulus durations of 1, 2, 5, 10, 20, 100, and 330ms were presented randomly using custom MATLAB code to drive square pulses from a National Instruments data acquisition card. Laser power was held constant throughout each trial, and was calibrated manually in each session to drive robust multi-unit spiking at short latency from TRN units. Each recording session consisted of 300-600 stimuli delivered at 0.5 Hz, lasting 5-10 minutes.

Data processing and analysis

Neural data was filtered for spikes at 300-6000Hz. These signals were processed offline using custom MATLAB code. Spikes were sorted using simpleclust (https://github.com/open-ephys/simpleclust), and light-evoked artifacts were identified and rejected during this process based on characteristic shape and amplitude.

Multi-unit activity (MUA) was characterized by taking the RMS power of the filtered (300Hz-6000Hz) electrode signal and thresholding at 3 standard deviations above baseline

to detect events. MUA activity peaks with a duration greater than 16.5 ms (500 Neuralynx samples) was defined as a 'burst', and shorter events were excluded. Single-unit bursts were defined as three or more spikes separated by 4 ms or less, and preceded by a non-firing period of at least 100 ms (Swadlow and Gusev, 2001).

The durations of spiking responses to stimuli were determined from mean PSTHs using a morphologically inspired filter to define epochs of firing above baseline while ignoring brief (<3 ms) fluctuations. The duration of a PSTH response was determined by first detecting response epochs that were 3 standard deviations above mean pre-stimulus activity (20 ms). The duration was then defined as sustained increases with no longer than a 3 millisecond period without a threshold crossing.

Results

Longer optical stimulations increased burst probability and decreased burst latency

Successful optogenetic activation of TRN was defined as single unit spikes driven within 5 ms of stimulus onset, with spiking probability above 3 SD from the baseline mean of the PSTH. Electrode channels containing at least one well-defined single unit activated in this way were considered located in TRN for subsequent multi-unit activity (MUA) analyses (N = 60 sites, 7 mice).

Changing the duration of light stimulation increased the likelihood of subsequent bursts after the initial MUA response. An MUA 'burst' was defined as a peak in MUA power at least 3 SD above the mean, excluding the time of stimulation to avoid light artifacts, and lasting at least 16.5 ms. As shown in the example plot in **Figure 2**, subsequent MUA bursts were observed following a pause of 100-300 ms after the initial light-driven response. In some cases, multiple subsequent MUA bursts were observed. In **Figure 2**, *blue* periods indicate initial firing, *green* indicates the first post-light burst, *orange* the second post-light burst, and *red* the third post-light burst.

With increasing optical duration, the likelihood of a subsequent burst and the probability of observing more than one subsequent burst were increased, and the latency to the first burst after light cessation was decreased. **Figure 3A-B** shows quantification of these dependencies. Chi-squared tests were performed for each pair of stimulus durations of most similar length (e.g., 2 versus 5 ms duration), and in each case the increase in proportion of trials exhibiting bursts following longer stimulation was statistically significant ($p < .05$). Linear regression of event probability on log stimulus duration was also statistically significant ($r^2 = .15$, $p < .01$).

Increased stimulus duration was also associated with a weak but steady decrease in the latency of MUA bursts from time of stimulation, as modeled by a linear regression on log stimulus duration (**Figure 4**, slope = -1796, $r^2 = .152$, $p < .05$ versus the constant model). In sum, longer TRN depolarizations increase the likelihood and decrease the delay before an MUA burst is observed.

We also analyzed single unit responses to light presentation. We isolated 100 single units that showed short-latency evoked activity (<5 milliseconds following light onset). To analyze single unit burst probability, bursting was defined similarly to Swadlow (Swadlow and Gusev, 2001) as a unit firing multiple spikes separated by less than 4 ms with a preceding quiescent period of at least 100 ms. An example raster plot from one recorded unit is shown in **Figure 5**, with detected bursts indicated using the same color scheme as **Figure 2**. Highly synchronized firing at stimulus onset was selected for by our rules for the inclusion of responsive units, as with the MUA analyses, following analyses exclude the initial response in quantification of 'second' bursts in single units.

Burst probability increased with stimulus duration in isolated single units (**Figure 6**), and these differences were characterized by a linear regression of burst frequency versus log stimulus duration ($r^2 = .09$, $p < .01$). Single unit burst latency was highly variable, but there was a weak linear relationship between increased stimulus duration and lower latency to bursts across single units ($r^2 = .01$, $P < .01$).

Distinct response types emerge with increasing duration of TRN depolarization

Inspection of the PSTHs evoked by light stimuli ranging from 2–100 ms duration for all activated single units suggested the existence of distinct sub-populations. This response within the population can be appreciated by examination of two specific examples. significant diversity existed in the light pulse required to reach this plateau. In **Figure 7A**,

the cell on the *left* showed robust firing lasting ~20 milliseconds for all light durations of 5 ms or greater. In contrast, the cell on the *right* showed a basically linear increase in the duration of firing with the duration of light, reaching a 20 ms response duration when a 20 ms light pulse was applied. To visualize these data, we calculated the duration of firing as contiguous activity 3SD or greater over baseline (ignoring gaps of up to 3 ms) and plotted the data as a line plot connecting the responses of each individual cell. All neurons showed sustained firing (> 20 ms duration) following sustained optical drive (**Figure 7B**). However, as indicated by the examples, there was significant diversity as to the light duration required to reach this response. The *red* and *blue* lines in **Figure 7B** correspond to the example cells shown in **Figure 7A**.

To visualize this diversity in the data in a more reduced format, we plotted response duration histograms for all neurons as a function period of light drive (**Figure 7C**). In the range from 2-20 milliseconds, a clearly bimodal distribution is observed, with a prominent peak of neurons with 20 millisecond durations of firing across stimulus conditions, and a second contingent with shorter sustained responses for shorter stimuli.

The summary plots revealed a separation into two main groups in response to stimulus durations. Due to large variability and difficulty of distinguishing evoked from spontaneous spikes in the 2 ms condition, the range between 5 ms and 20 ms was chosen for further analysis. Linear regressions were fit for the response lengths of each cell to quantify the relationship between stimulus and response durations. We measured the relative slope of responses in this region of the curve and found that these formed an apparently bimodal

distribution (**Figure 8A**), which we separated into two categories using a Gaussian mixture model. This distribution was modeled as a combination of two Gaussians in one dimension, with the best fit containing the following components (distribution 1: mean = -.13, standard deviation = .07; distribution 2: mean = .90, standard deviation = .10; slope at crossover = .35).

We next plotted the firing rate PSTHs for each group, and these are shown in **Figure 8B**. This population level spiking format reveals the main effects observed in the rest of the data, that linear cells fire less to briefer stimuli, whereas non-linear cells show more sustained responses up to a duration of ~20 milliseconds.

We next investigated whether intrinsic activity patterns and/or excitability separated these groups (**Figure 8C-D**). Spontaneous firing rate was statistically indistinguishable between these groups (linear = 0.47 spikes/s, SD = 1.0; nonlinear = 0.85, SD = 2.3; two-tailed Wilcoxon ran-sum test, $p = .56$). In contrast, mean evoked firing during light presentation was higher for the non-linear cells (summed across all light intensity levels; linear = 2.2 spikes/s, nonlinear = 4.8 spikes/s, two-tailed Wilcoxon rank-sum test, $p < .05$). Significant differences were also found in evoked burst rate, as non-linear ceils were approximately two times more likely to burst during stimulation than linear cells (linear = 0.15 bursts/s, nonlinear = 0.31 bursts/s, two-tailed Wilcoxon rank-sum test, $p<.05$).

One possibility is that higher overall excitability differences between the two groups could be reflected in the likelihood of observing an extracellularly defined burst. To test whether

these burst rate differences were a product of overall excitability, subgroups of each unit class were matched for driven spike rate and reanalyzed (**Figure 8C**, third panel). Cells in both groups were sorted in order of mean evoked spike rate – linear cells had a wider range, so the minimum and median values of the nonlinear group were taken as boundaries for extracting a subset of the linear group. The mean evoked firing rates of these extracted subgroups were statistically indistinguishable (N = 18 linear cells, 22 nonlinear; linear = 2.8 sp/s, nonlinear = 3.0 sp/s, two-tailed Wilcoxon rank-sum test, p = 0.78). These subsets maintained a significant distinction in burst firing (linear = 0.15 bursts/s, nonlinear = 0.28 bursts/s, two-tailed Wilcoxon rank-sum test, $p<.05$), and the behavior of these sub-populations was indistinguishable from the values in each category (linear subset vs linear population, p = .13, nonlinear subset versus population, p = .30).

Discussion

In this study, we characterized the response of TRN cells to optogenetic stimuli of varying durations *in vivo*. In the lightly-anesthetized mouse, TRN was mostly quiescent in spontaneous spiking and oscillatory activity. Optical drive not only directly stimulated firing, but also post-stimulus activity that persisted for up to hundreds of milliseconds. We found that this response was dependent on total stimulus duration, as stimulation for 100 ms or longer consistently evoked subsequent bursting, while less than 10 ms stimulation was ineffective at post-stimulus burst induction. In contrast, persistence of directly driven firing could be observed after stimulus offset in a subset of recorded units. These 'nonlinear' cells also displayed a higher rate of evoked bursting.

The steep increase in the probability of evoking a subsequent burst after light cessation at durations of 10 ms or longer (**Figure 3A**) suggests that endogenous depolarizing events of at least this duration may be key to triggering rhythmic TRN activity. As previously described, the TRN receives input from multiple structures across a wide range of durations. Such depolarization could be driven by burst input from relay cells, or by sustained tonic relay firing reflecting strong bottom-up sensory input. Projections from the prefrontal cortex to the TRN are widespread with large axon boutons in the primate (Zikopoulos and Barbas, 2006), and recent work from Wimmer et al. (Wimmer et al., 2015) described potent modulation of TRN in mice following optogenetic stimulation of the rodent analogue to PFC. This projection could induce lasting activity in the TRN as a function of behavioral demands. Biophysically, Neyer et al. (Neyer et al., 2016) have demonstrated that mGluR agonists can trigger the release of calcium from intracellular stores in TRN, leading to long-lasting depolarization. In sum, our data predict that minimally 10 milliseconds of depolarization is required to evoke bursting, but that there are many possible candidates for generating this input.

The two types of responses observed here may reflect the basic physiological observations of Contreras et al. (Contreras et al., 1992) in urethane-anesthetized cats. Their type I cells showed bursting, much as our non-linear cells showed a greater propensity to burst. In contrast, their type II cells did not burst but did show a linear increase in firing with sustained depolarization, and our linear cells showed a diminished burst rate relative to non-linear cells but a closer mapping between stimulus duration and spiking period. In spite of these similarities, there are clear differences in our present findings. In the

Contreras data, ~ 20% of recorded cells were classified as 'type II', but we found approximately the same number of linear and nonlinear cells. This difference could reflect the respective sampling biases for intracellular versus extracellular recording, or could indicate that these are separate phenomena. More importantly, type II neurons were not observed to fire in bursts, either on release from hyperpolarization or from depolarizing pulses given to cells held at extremely hyperpolarized levels. This behavior suggests a lack of t-type calcium channels, as opposed to our linear cells that have a lower burst rate, but do display this pattern of activity to some extent.

Different modes of burst firing could arise from the intrinsic mechanisms underlying membrane bistability observed during spindles in a subpopulation of TRN cells (Fuentealba et al., 2005). This effect was hypothesized to require voltage-gated Na+ channels, and did not include abolition of burst firing. In our preparation, however, sustained spindle-like activity was not observed. These observations are consistent with earlier work using isoflurane during dLGN and V1 recordings in mice (Denman and Contreras, 2015). That study used an isoflurane concentration of ~1.2% during recordings to produce an anesthetized state with minimal slow oscillations in cortex and strong L6 responses to stimulation. As the slow oscillation is thought to be key for synchronizing thalamically-generated spindles (Steriade, 2001), the absence of obvious rhythmicity in our data may be a product of the relatively light (0.9%-1.1%) isoflurane levels during recording sessions.

The cell classes observed here may also reflect those reported by Halassa et al. (Halassa et al., 2014). The more readily-bursting 'non-linear' cells that fired at higher evoked rates in our anesthetized preparation may correspond to those units previously reported with high firing rates positively correlated to spindles and delta oscillations. In contrast, the 'linear' neurons observed here that did not burst as readily may correspond to those TRN neurons more active in aroused states, potentially indicative of more tonic firing patterns. One caveat to this interpretation is that the populations described by Halassa et al. were distinguished by projection targets, and were also distributed unevenly along the anterior-posterior axis of the TRN. The segment of the TRN targeted in our study was consistently posterior to the area of overlap between limbic- and sensory-projecting TRN cells described in this previous work.

There are a number of potential explanations for distinct classes of activity in TRN units. One possibility is that the differences observed reflect subtle shift in state of the animal within the regime of anesthesia employed here. We do not favor this view, as animals showed little variation in basic measures of state while under a fairly tight range of administered anesthetic levels, which were consistent with levels used previously to obtain an EEG-activated pattern (Denman and Contreras, 2015). More importantly, 'linear' and 'nonlinear' cells were observed during the same recordings, suggesting that their behavior does not reflect an overall shift in arousal or baseline state between sessions or animals. Additionally, matching cells from each group for evoked firing rates did not change the observed difference in likelihood of burst induction.

Functional differences of this sort could be explained by intrinsic biophysical heterogeneity in the somatosensory TRN. Differences in responses could also be due to differing patterns of connectivity between groups of TRN cells. Anatomical evidence of heterogeneous morphology (Pinault and Deschênes, 1998a; 1998b; Desîlets-Roy et al., 2002) and laminar distribution of cells based on thalamic target (Clemence and Mitrofanis, 1992; Pinault and Deschênes, 1998a; 1998b; Desîlets-Roy et al., 2002) suggests the possibility of neurons within the same area of TRN participating in different thalamocortical circuits.

We also observed suppressed units on TRN responsive contacts. Out of 186 total recorded single units, 60 showed initial response suppression with light drive, and 26 showed no response. Because suppressive and absent responses could not be classified as emerging from TRN cells with the same certitude as quickly responding activated units, they were excluded from the current analysis. These units may represent a mixture of TRN cells and axons of passage from relay nuclei. Because all TRN cells are inhibitory and should express ChR2 in the VGAT mouse, we would expect suppression of TRN neurons could result from the activation of intra-TRN connections or inhibitory axon terminals for exogenous sources (e.g., the basal ganglia). The strength and timing of inhibitory input combined with differential levels of direct optogenetic drive (due to ChR2 expression levels or light propagation) could generate a primarily suppressive effect or excitation followed by rapid suppression, both of which we observed in a subset of recordings. If these units represent relay axons, there could be more complex circuit interactions, but the most straightforward interpretation is that we were seeing the effect of monosynaptic inhibition.

We did not observe sustained slow wave (1-3 Hz) or spindling activity in the spiking at specific locations in the TRN activated by discrete light presentation. Even under the most favorable light pulse conditions ($\geq$ 100 millisecond stimulation), 2 or more bursts in the MUA were observed only <25% of the time, and the probability was much lower for single units (6–7%). That said, the initial period from first response to subsequent burst was 100-300 milliseconds, indicating a 'one cycle' rhythmicity of 3-10 Hz falling within the high range of slow wave activity and within the typical spindle frequency range (Steriade et al., 1985; Steriade and Llinás, 1988; Beenhakker and Huguenard, 2009).

The failure to observe slow waves or spindles in the spiking of specific units or positions, despite observation of discrete neocortical slow waves following sustained optogenetic TRN activation in a similar model (Lewis et al., 2015) and neocortical spindles following discrete TRN optogenetic activation (Halassa et al., 2011), could result from several factors. We analyzed expression at single positions in the TRN, reflecting the linear array we employed in these studies. Potentially, lateral propagation and expression of later bursts at different positions in TRN and in relay nuclei will occur. Initial TRN activation will evoke suppression and rebound bursting in VPm (Halassa et al., 2011) that will then activate and drive feedback from the neocortex as part of rhythm maintenance, potentially at 'off beam' locations not topographically aligned with the initiating TRN position. The anesthetized state of the mouse in our studies could also have an effect on burst firing and rhythmicity after stimulation. The use of isoflurane allowed for rapid titration of anesthetic depth, but it has been shown to cause depolarization in TRN cells (Joksovic and Todorovic, 2010) while inhibiting both tonic and burst firing. Isoflurane levels in this study were kept low during

recording sessions, but it is possible in the awake mouse or during natural slow-wave sleep that bursting and spindle-like oscillations would be more frequent.

Acknowledgements: This work was supported by NIH RO1 NS045130 and NSF grant 1131850.

References

Astori S, Wimmer RD, Prosser HM, Corti C, Corsi M, Liaudet N, Volterra A, Franken P, Adelman JP, Lüthi A. The Ca(V)3.3 calcium channel is the major sleep spindle pacemaker in thalamus. *Proceedings of the National Academy of Sciences* 108: 13823–13828, 2011.

Austin CP, Ky B, Ma L, Morris JA, Shughrue PJ. Expression of Disrupted-In-Schizophrenia-1, a schizophrenia-associated gene, is prominent in the mouse hippocampus throughout brain development. *Neuroscience* 124: 3–10, 2004.

Avanzini G, de Curtis M, Franceschetti S, Sancini G, Spreafico R. Cortical versus thalamic mechanisms underlying spike and wave discharges in GAERS. *Epilepsy Res* 26: 37–44, 1996.

Bal T, Krosigk von M, McCormick DA. Synaptic and membrane mechanisms underlying synchronized oscillations in the ferret lateral geniculate nucleus in vitro. *J Physiol (Lond)* 483 (Pt 3): 641–663, 1995.

Bal T, McCormick DA. Mechanisms of oscillatory activity in guinea-pig nucleus reticularis thalami in vitro: a mammalian pacemaker. *J Physiol (Lond)* 468: 669–691, 1993.

Beenhakker MP, Huguenard JR. Neurons that fire together also conspire together: is normal sleep circuitry hijacked to generate epilepsy? *Neuron* 62: 612–632, 2009.

Boucetta S, Cissé Y, Mainville L, Morales M, Jones BE. Discharge profiles across the sleep-waking cycle of identified cholinergic, GABAergic, and glutamatergic neurons in the pontomesencephalic tegmentum of the rat. *J Neurosci* 34: 4708–4727, 2014.

Bourassa J, Pinault D, Deschênes M. Corticothalamic projections from the cortical barrel field to the somatosensory thalamus in rats: a single-fibre study using biocytin as an anterograde tracer. *Eur J Neurosci* 7: 19–30, 1995.

Castro-Alamancos MA, Connors BW. Spatiotemporal properties of short-term plasticity sensorimotor thalamocortical pathways of the rat. *Journal of Neuroscience* 16: 2767–2779, 1996.

Castro-Alamancos MA. Different temporal processing of sensory inputs in the rat thalamus during quiescent and information processing states in vivo. *J Physiol (Lond)* 539: 567–578, 2002.

Clemence AE, Mitrofanis J. Cytoarchitectonic heterogeneities in the thalamic reticular nucleus of cats and ferrets. *J Comp Neurol* 322: 167–180, 1992.

Contreras D, Dossi RC, Steriade M. Bursting and tonic discharges in two classes of reticular thalamic neurons. *J Neurophysiol* 68: 973–977, 1992.

Cox CL, Huguenard JR, Prince DA. Heterogeneous axonal arborizations of rat thalamic reticular neurons in the ventrobasal nucleus. *J Comp Neurol* 366: 416–430, 1996.

Crandall SR, Cruikshank SJ, Connors BW. A corticothalamic switch: controlling the thalamus with dynamic synapses. *Neuron* 86: 768–782, 2015.

Crick F. Function of the thalamic reticular complex: the searchlight hypothesis. *Proc Natl Acad Sci USA* 81: 4586–4590, 1984.

Crunelli V, Cope DW, Terry JR. Transition to absence seizures and the role of GABA(A) receptors. *Epilepsy Res* 97: 283–289, 2011.

Crunelli V, Lightowler S, Pollard CE. A T-type Ca2+ current underlies low-threshold Ca2+ potentials in cells of the cat and rat lateral geniculate nucleus. *J Physiol (Lond)* 413: 543–561, 1989.

Diamond ME, Armstrong-James M, Ebner FF. Somatic sensory responses in the rostral sector of the posterior group (POm) and in the ventral posterior medial nucleus (VPM) of the rat thalamus. *J Comp Neurol* 318: 462–476, 1992.

de Curtis M, Spreafico R, Avanzini G. Excitatory amino acids mediate responses elicited in vitro by stimulation of cortical afferents to reticularis thalami neurons of the rat. *Neuroscience* 33: 275–283, 1989.

Denman DJ, Contreras D. Complex Effects on In Vivo Visual Responses by Specific Projections from Mouse Cortical Layer 6 to Dorsal Lateral Geniculate Nucleus. *J Neurosci* 35: 9265–9280, 2015.

Desîlets-Roy B, Varga C, Lavallée P, Deschênes M. Substrate for cross-talk inhibition between thalamic barreloids. *J Neurosci* 22: RC218, 2002.

Ferrarelli F, Huber R, Peterson MJ, Massimini M, Murphy M, Riedner BA, Watson A, Bria P, Tononi G. Reduced sleep spindle activity in schizophrenia patients. *Am J Psychiatry* 164: 483–492, 2007.

Ferrarelli F, Peterson MJ, Sarasso S, Riedner BA, Murphy MJ, Benca RM, Bria P, Kalin NH, Tononi G. Thalamic dysfunction in schizophrenia suggested by whole-night deficits in slow and fast spindles. *Am J Psychiatry* 167: 1339–1348, 2010.

Fuentealba P, Timofeev I, Bazhenov M, Sejnowski TJ, Steriade M. Membrane bistability in thalamic reticular neurons during spindle oscillations. *J Neurophysiol* 93: 294–304, 2005.

Gandia J, Delasheras S, Garcia M, Gimenezamaya J. Afferent projections to the reticular thalamic nucleus from the globus pallidus and the substantia nigra in the rat. *Brain Research Bulletin* 32: 351–358, 1993.

Golshani P, Liu XB, Jones EG. Differences in quantal amplitude reflect GluR4- subunit number at corticothalamic synapses on two populations of thalamic neurons. *Proc Natl Acad Sci USA* 98: 4172–4177, 2001.

Halassa MM, Chen Z, Wimmer RD, Brunetti PM, Zhao S, Zikopoulos B, Wang F, Brown EN, Wilson MA. State-dependent architecture of thalamic reticular subnetworks. *Cell* 158: 808–821, 2014.

Halassa MM, Siegle JH, Ritt JT, Ting JT, Feng G, Moore CI. Selective optical drive of thalamic reticular nucleus generates thalamic bursts and cortical spindles. *Nat Neurosci* (July 24, 2011). doi: 10.1038/nn.2880.

Huguenard JR, McCormick DA. Thalamic synchrony and dynamic regulation of global forebrain oscillations. *Trends Neurosci* 30: 350–356, 2007.

Huguenard JR, Prince DA. A novel T-type current underlies prolonged Ca(2+)-dependent burst firing in GABAergic neurons of rat thalamic reticular nucleus. *Journal of Neuroscience* 12: 3804–3817, 1992.

Joksovic PM, Todorovic SM. Isoflurane modulates neuronal excitability of the nucleus reticularis thalami in vitro. *Ann N Y Acad Sci* 1199: 36–42, 2010.

Jones EG. Some aspects of the organization of the thalamic reticular complex. *J Comp Neurol* 162: 285–308, 2004.

Kimura A, Imbe H. Anatomically structured burst spiking of thalamic reticular nucleus cells: implications for distinct modulations of sensory processing in lemniscal and non-lemniscal thalamocortical loop circuitries. *Eur J Neurosci* 41: 1276–1293, 2015.

Kwegyir-Afful EE, Simons DJ. Subthreshold receptive field properties distinguish different classes of corticothalamic neurons in the somatosensory system. *J Neurosci* 29: 964–972, 2009.

Lam Y-W, Sherman SM. Functional organization of the somatosensory cortical layer 6 feedback to the thalamus. *Cereb Cortex* 20: 13–24, 2010.

Lam Y-W, Sherman SM. Functional organization of the thalamic input to the thalamic reticular nucleus. *J Neurosci* 31: 6791–6799, 2011.

Landisman CE, Connors BW. VPM and PoM nuclei of the rat somatosensory thalamus: intrinsic neuronal properties and corticothalamic feedback. *Cereb Cortex* 17: 2853–2865, 2007.

Lee S-C, Patrick SL, Richardson KA, Connors BW. Two functionally distinct networks of gap junction-coupled inhibitory neurons in the thalamic reticular nucleus. *J Neurosci* 34: 13170–13182, 2014.

Lee S-H, Govindaiah G, Cox CL. Heterogeneity of firing properties among rat thalamic reticular nucleus neurons. *J Physiol (Lond)* 582: 195–208, 2007.

Lewis LD, Voigts J, Flores FJ, Schmitt LI, Wilson MA, Halassa MM, Brown EN. Thalamic

reticular nucleus induces fast and local modulation of arousal state. *Elife* 4, 2015.

Llinás RR, Ribary U, Jeanmonod D, Kronberg E, Mitra PP. Thalamocortical dysrhythmia: A neurological and neuropsychiatric syndrome characterized by magnetoencephalography. *Proc Natl Acad Sci USA* 96: 15222–15227, 1999.

Liu X-B, Murray KD, Jones EG. Low-threshold calcium channel subunit Ca(v) 3.3 is specifically localized in GABAergic neurons of rodent thalamus and cerebral cortex. *J Comp Neurol* 519: 1181–1195, 2011.

McAlonan K, Brown VJ, Bowman EM. Thalamic reticular nucleus activation reflects attentional gating during classical conditioning. *J Neurosci* 20: 8897–8901, 2000.

McAlonan K, Brown VJ. The thalamic reticular nucleus: more than a sensory nucleus? *Neuroscientist* 8: 302–305, 2002.

McAlonan K, Cavanaugh J, Wurtz RH. Attentional modulation of thalamic reticular neurons. *J Neurosci* 26: 4444–4450, 2006.

Mease RA, Krieger P, Groh A. Cortical control of adaptation and sensory relay mode in the thalamus. *Proceedings of the National Academy of Sciences* 111: 6798–6803, 2014.

Neyer C, Herr D, Kohmann D, Budde T, Pape H-C, Coulon P. mGluR-mediated calcium signalling in the thalamic reticular nucleus. *Cell Calcium* (March 28, 2016). doi: 10.1016/j.ceca.2016.03.009.

Paz JT, Davidson TJ, Frechette ES, Delord B, Parada I, Peng K, Deisseroth K, Huguenard JR. Closed-loop optogenetic control of thalamus as a tool for interrupting seizures after cortical injury. *Nat Neurosci* 16: 64–70, 2013.

Pinault D, Deschênes M. Anatomical evidence for a mechanism of lateral inhibition in the rat thalamus. *Eur J Neurosci* 10: 3462–3469, 1998a.

Pinault D, Deschênes M. Projection and innervation patterns of individual thalamic reticular axons in the thalamus of the adult rat: a three-dimensional, graphic, and morphometric analysis. *J Comp Neurol* 391: 180–203, 1998b.

Pinault D, Leresche N, Charpier S, Deniau J-MM, Marescaux C, Vergnes M, Crunelli V. Intracellular recordings in thalamic neurones during spontaneous spike and wave discharges in rats with absence epilepsy. *J Physiol (Lond)* 509 (Pt 2): 449–456, 1998.

Pinault D. The thalamic reticular nucleus: structure, function and concept. *Brain Research Reviews* 46: 1–31, 2004.

Pinault D. Dysfunctional thalamus-related networks in schizophrenia. *Schizophr Bull* 37: 238–243, 2011.

Pita-Almenar JD, Yu D, Lu H-C, Beierlein M. Mechanisms underlying desynchronization of

cholinergic-evoked thalamic network activity. *J Neurosci* 34: 14463–14474, 2014.

Pratt JA, Morris BJ. The thalamic reticular nucleus: a functional hub for thalamocortical network dysfunction in schizophrenia and a target for drug discovery. *J Psychopharmacol (Oxford)* 29: 127–137, 2015.

Rigas P, Castro-Alamancos MA. Thalamocortical Up states: differential effects of intrinsic and extrinsic cortical inputs on persistent activity. *J Neurosci* 27: 4261–4272, 2007.

Schizophrenia Working Group of the Psychiatric Genomics Consortium. Biological insights from 108 schizophrenia-associated genetic loci. *Nature* 511: 421–427, 2014.

Sherman SM, Guillery RW. Functional organization of thalamocortical relays. *J Neurophysiol* 76: 1367–1395, 1996.

Slaght SJ, Leresche N, Deniau J-MM, Crunelli V, Charpier S. Activity of thalamic reticular neurons during spontaneous genetically determined spike and wave discharges. *J Neurosci* 22: 2323–2334, 2002.

Steriade M. Impact of network activities on neuronal properties in corticothalamic systems. *J Neurophysiol* 86: 1–39, 2001.

Steriade M, Contreras D, Curró Dossi R, Nuñez A. The Slow (<1Hz) Oscillation in Reticular Thalamic and Thalamocortical Neurons: Scenario of Sleep Rhythm Generation in Interacting Thalamic and Neocortical Networks . *Journal of Neuroscience* 13: 3284–3299, 1993.

Steriade M, Deschênes M, Domich L, Mulle C. Abolition of spindle oscillations in thalamic neurons disconnected from nucleus reticularis thalami. *J Neurophysiol* 54: 1473–1497, 1985.

Steriade M, Llinás RR. The functional states of the thalamus and the associated neuronal interplay. *Physiol Rev* 68: 649–742, 1988.

Sun Q-Q, Huguenard JR, Prince DA. Somatostatin inhibits thalamic network oscillations in vitro: actions on the GABAergic neurons of the reticular nucleus. *J Neurosci* 22: 5374–5386, 2002.

Swadlow HA, Gusev AG. The impact of "bursting" thalamic impulses at a neocortical synapse. *Nat Neurosci* 4: 402–408, 2001.

Temereanca S, Simons DJ. Functional topography of corticothalamic feedback enhances thalamic spatial response tuning in the somatosensory whisker/barrel system. *Neuron* 41: 639–651, 2004.

Tringham E, Powell KL, Cain SM, Kuplast K, Mezeyova J, Weerapura M, Eduljee C, Jiang X, Smith P, Morrison J-L, Jones NC, Braine E, Rind G, Fee-Maki M, Parker D, Pajouhesh

H, Parmar M, O'Brien TJ, Snutch TP. T-type calcium channel blockers that attenuate thalamic burst firing and suppress absence seizures. *Sci Transl Med* 4: 121ra19, 2012.

Weese GD, Phillips JM, Brown VJ. Attentional orienting is impaired by unilateral lesions of the thalamic reticular nucleus in the rat. *J Neurosci* 19: 10135–10139, 1999.

Wimmer RD, Schmitt LI, Davidson TJ, Nakajima M, Deisseroth K, Halassa MM. Thalamic control of sensory selection in divided attention. *Nature* (October 21, 2015). doi: 10.1038/nature15398.

Yu X-J, Xu X-X, He S, He J. Change detection by thalamic reticular neurons. *Nat Neurosci* 12: 1165–1170, 2009.

Zikopoulos B, Barbas H. Prefrontal projections to the thalamic reticular nucleus form a unique circuit for attentional mechanisms. *J Neurosci* 26: 7348–7361, 2006.

Figures

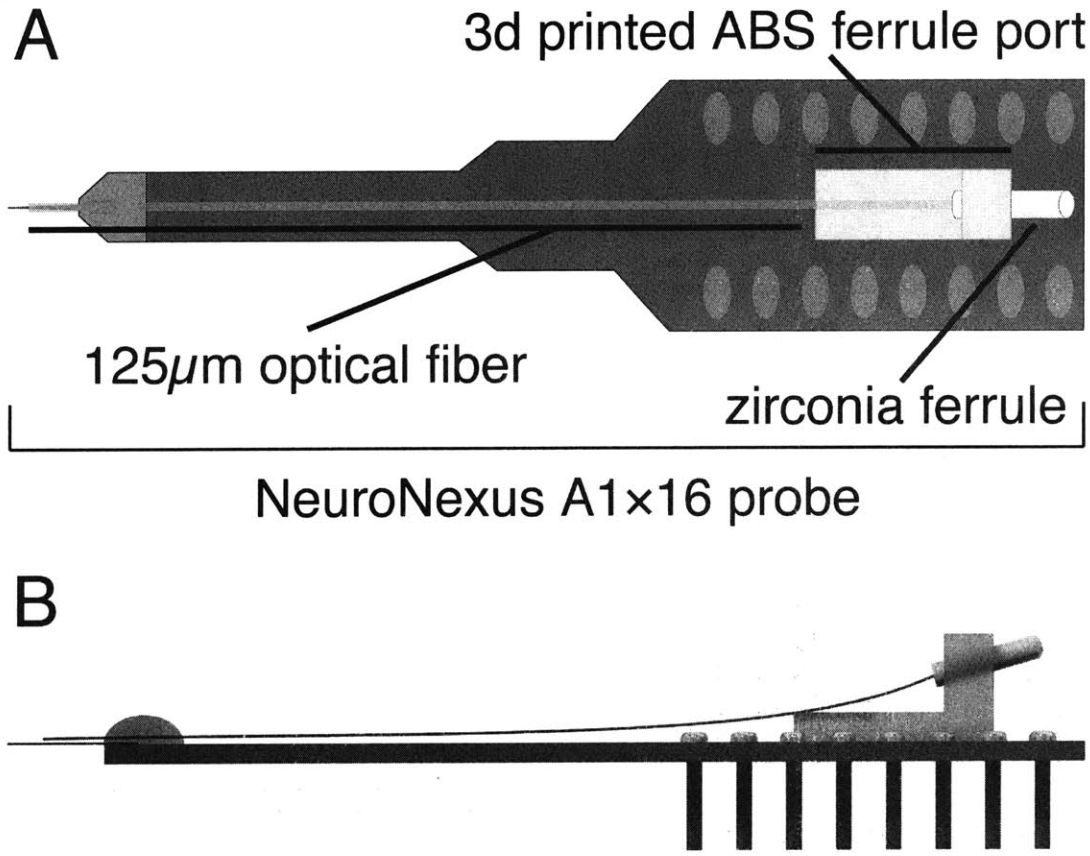

Figure 1

Diagram of custom optrodes used for all recordings

A. The base electrode used was a Neuronexus laminar probe with 16 contacts at 25μm separation (model: A1x16-5mm-25-177-A16). A 105μm core/125 μm diameter optical fiber (Thorlabs, Glass Clad Silica Multimode fiber, 0.22NA) was positioned 200μm from the top recording site and fitted with a zirconia ferrule for attachment to laser output. B. CAD model of optrode design, showing fiber and ferrule configuration. The angle of the fiber bend was significantly below the minimal tolerated bend axis of the fiber, calculated as the radius of a circle 240 x the diameter of the fiber (30 mm).

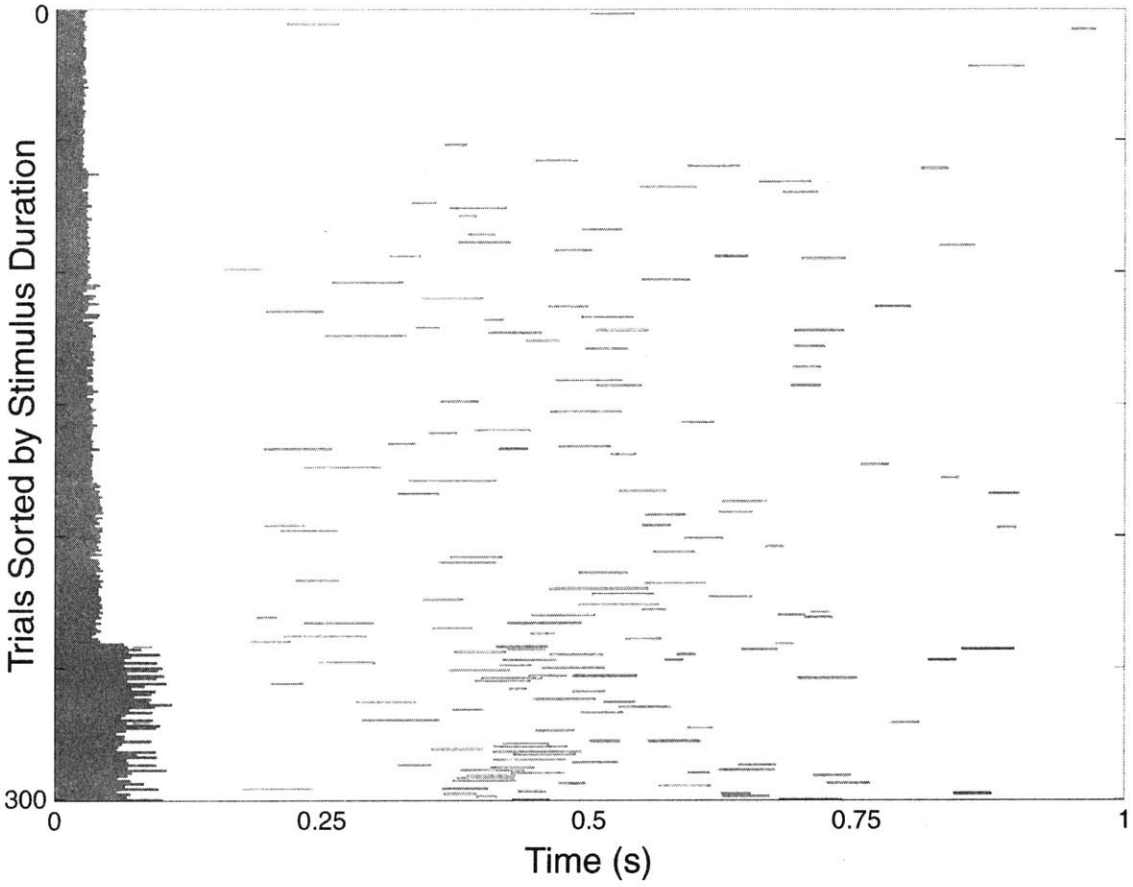

Figure 2

Multi-unit burst-like events after light cessation increased in probability and decreased in latency with longer optical stimulus durations: Example session

Extracted multi-unit events from one electrode site in a given session are shown, with responses ordered by stimulus duration from *top* (shortest, 2 milliseconds duration) to *bottom* (longest, 100 milliseconds duration). Events were defined as sustained periods (> 16.5 milliseconds) in which firing exceeded a threshold of 3 standard deviations from the mean activity rate (see Methods for details). *Dark blue horizontal bars* indicate firing overlapping with the period of optical stimulus presentation. Other colors indicate events occurring after light cessation: *Green* initial event; *Orange* second event; *Red* third event.

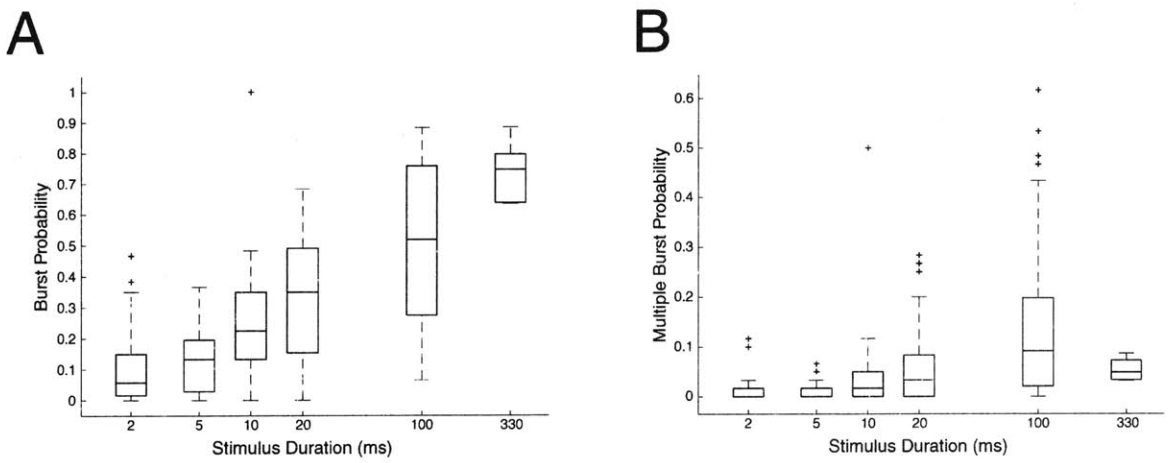

Figure 3

Multi-unit burst-like events after light cessation increased in probability and decreased in latency with longer optical stimulus durations: Population analyses

A. Across 60 multi-unit sites tested with multiple optical stimulus durations, the probability of multi-unit burst-like events increased with stimulus duration (N = 60 multi-unit sites; $r^2 = 0.37$; $p < .01$). B. The probability of observing more than one multi-unit burst like event in the period up to 1 second following light cessation increased linearly with log stimulus duration ($r^2 = 0.15$; $p < .01$). Boxes represent 1st and 3rd quartiles of the sample data, with the median value indicated by a line. Whiskers extend to the maximum and minimum data points for values up to 1.5 times the interquartile range below the 1st quartile or above the 3rd quartile. Points beyond this range are indicated by the (+) symbol.

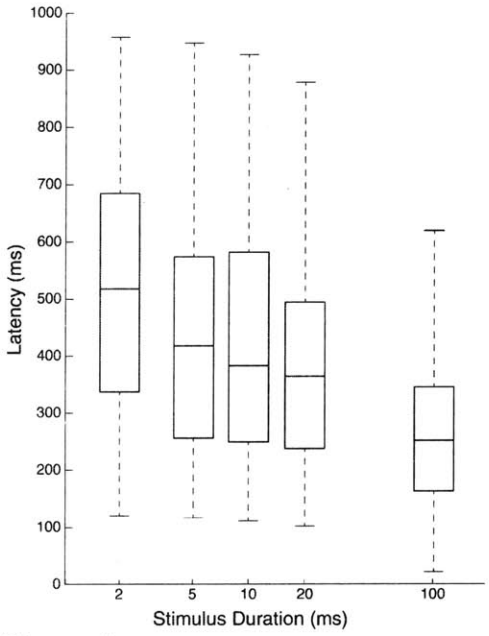

Figure 4

Latency of multi-unit burst-like events following stimulus offset decreased as a function of stimulus duration.

Boxes represent 1st and 3rd quartiles of the sample data, with the median value indicated by a line. Whiskers extend to the maximum and minimum data points for values up to 1.5 times the interquartile range below the 1st quartile or above the 3rd quartile. Points beyond this range are indicated by the (+) symbol. A linear relationship was present between latency and stimulus duration ($r^2 = 0.152$, p-value versus constant model <.05).

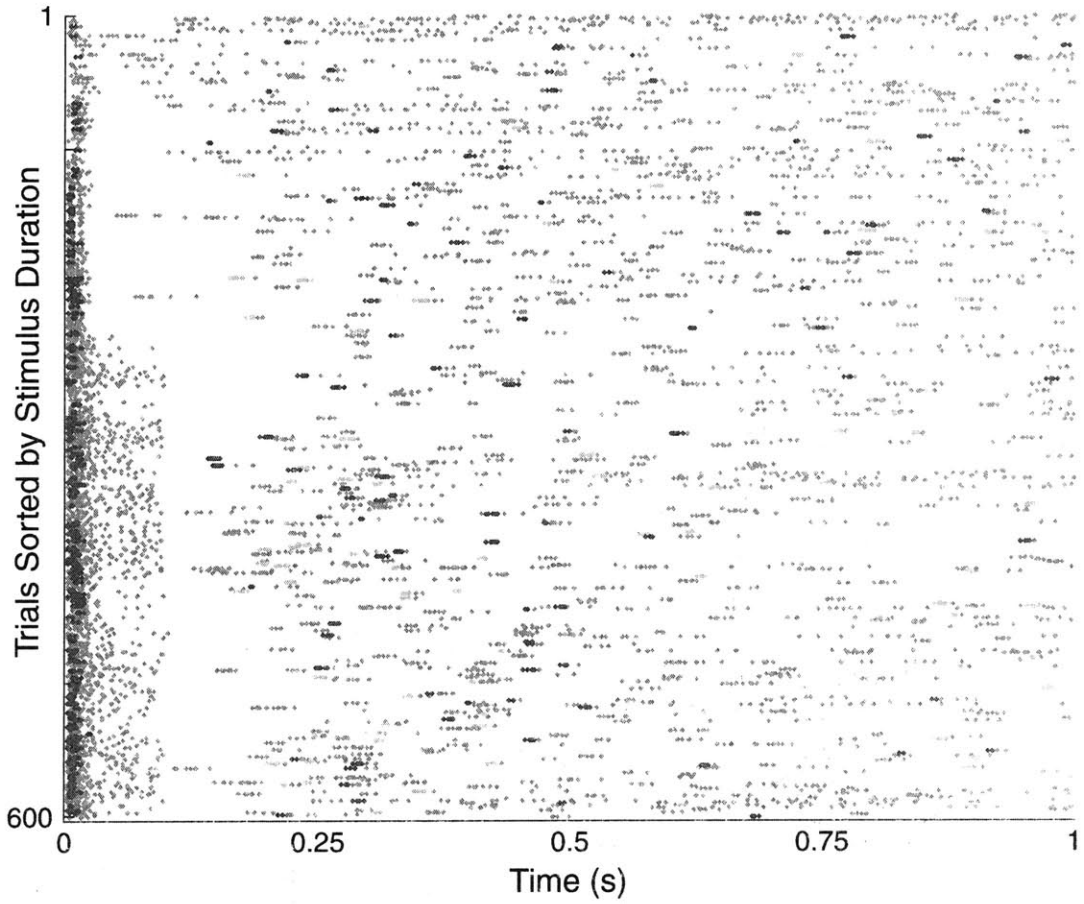

Figure 5

Single unit bursting after light cessation increased in probability and decreased in latency with longer optical stimulus durations: Example session

Extracted bursts from one example sorted unit in a given session are shown, with responses ordered by stimulus duration from *top* (shortest, 2 milliseconds duration) to *bottom* (longest, 100 milliseconds duration). Bursts were classified as spikes with a 4ms or less inter-spike interval, preceded by at least 100ms of silence (see Methods for details). *Gray dots* indicate single spikes. *Dark blue dots* indicate the first extracted burst for a given stimulus (many occurring during the stimulation period). Other colors indicate bursts occurring after light cessation: *Green* second burst; *Orange* third burst.

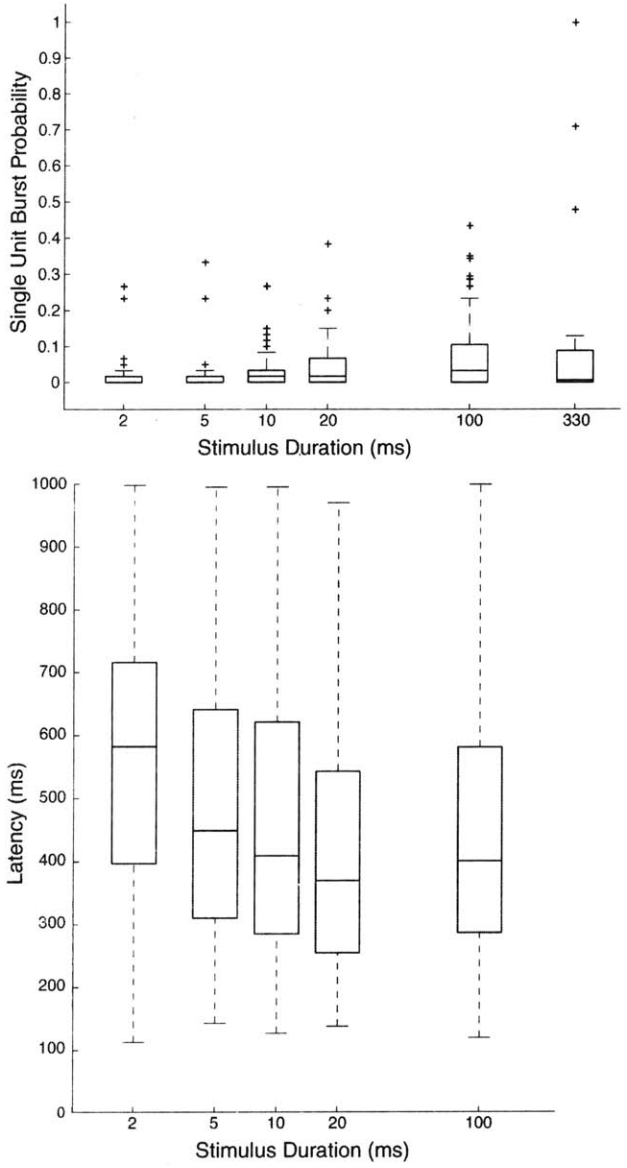

Figure 6

Probability of bursting in single units after light cessation increased with stimulus duration

Top A box and whisker plot showing the proportion of trials containing one or more single unit bursts in the period following stimulus offset at increasing stimulus durations. (linear regression $r^2 = .09$, $p < .01$). *Bottom* A linear trend was observed for burst latency ($r^2 = .01$,

$p < .01$). Boxes represent 1st and 3rd quartiles of the sample data, with the median value indicated by a line. Whiskers extend to the maximum and minimum data points for values up to 1.5 times the interquartile range below the 1st quartile or above the 3rd quartile. Points beyond this range are indicated by the (+) symbol.

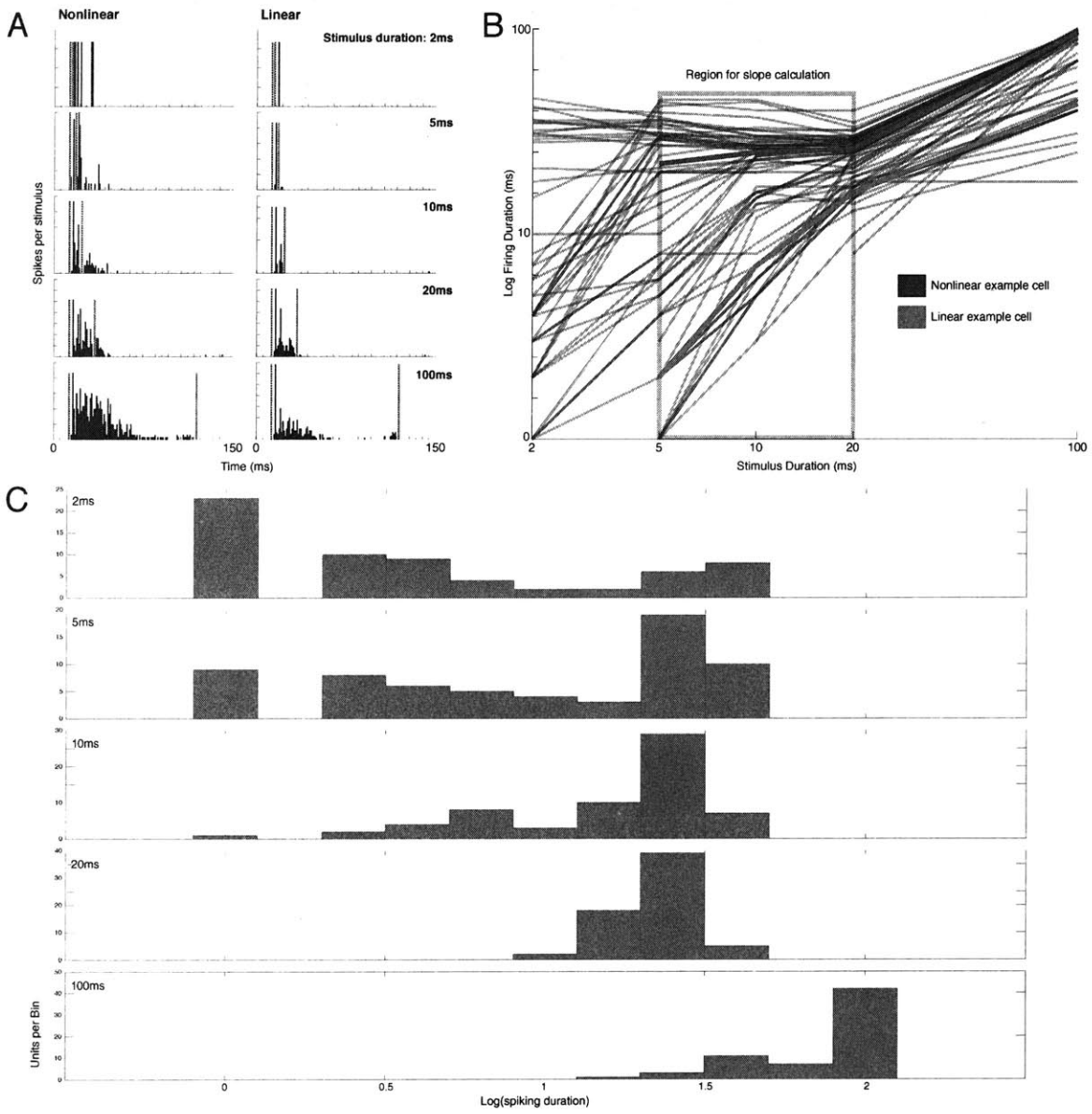

Figure 7

Two classes of cells are defined by the relationship of stimulus duration to response duration. A. Example PSTHs sorted by stimulus duration for a 'nonlinear' and 'linear' cell. Red lines indicate stimulus onset and offset. Duration of firing was calculated from the PSTH by measuring the number of contiguous bins (with an allowance for gaps of up to

3ms) with activity 3 standard deviations or more above the pre-stimulus baseline. Overall duration of increased firing for the nonlinear unit is relatively stable between 5 and 20 ms stimulations. B. Stimulus duration versus firing duration plotted for all tested single units. Example units from (A) are highlighted (Nonlinear in blue, linear in red). Due to adaptation effects at the 100ms stimulus, slopes were calculated via linear fits of the data between 5ms and 20ms for all cells. C. Histograms of firing duration for all units at different stimulus durations show an overall trend towards longer responses. For shorter stimuli, the separation between linear and nonlinear groups is apparent in the distribution of responses including low duration bins (brief spiking in linear cells) and responses lasting tens of milliseconds (peak near 1.5 on log scale, ~32ms).

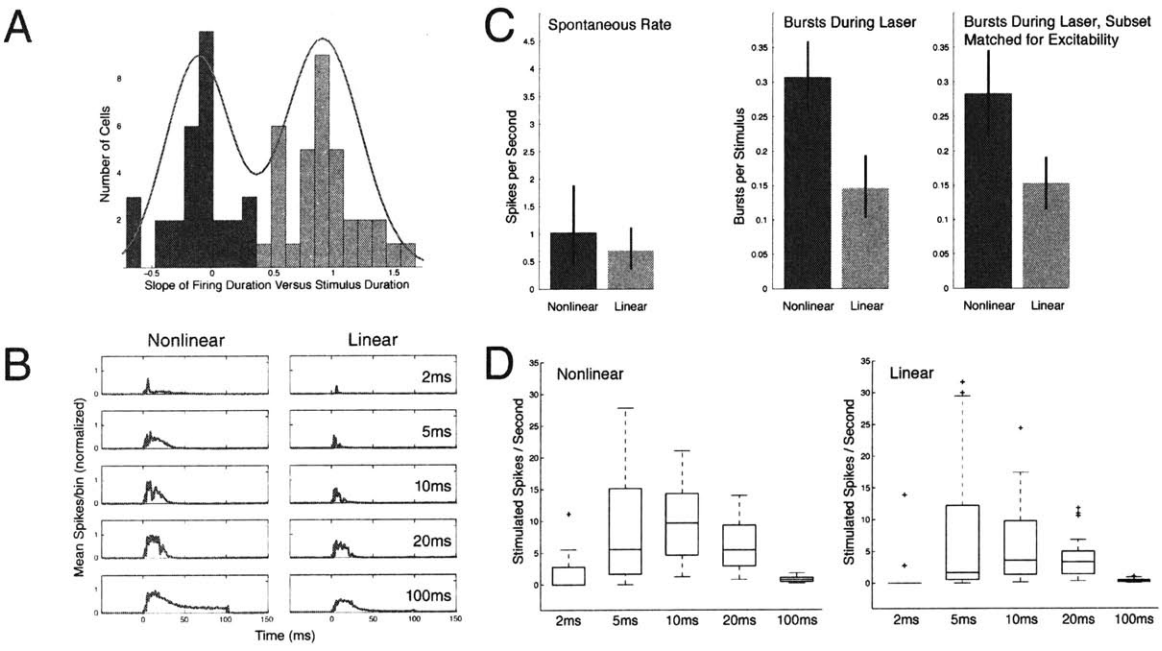

Figure 8

A. Histogram of slopes derived from data in 7B shows bimodality. Slope data were modeled as a mixture of two Gaussians in one dimension, and the minimum between modes used as the threshold between cell categories. B. Linear units (n=32) fire primarily during direct stimulation, while nonlinear units (n=33) exhibit prolonged activity even at short stimulus durations. Evoked firing rates are higher in the nonlinear group than in the linear group, but at 100ms of stimulation, the firing duration of both types is limited to the stimulus period and shows rate adaptation. C. Cell categories do not differ in spontaneous activity, but nonlinear units are more prone to burst. Right panel: units from linear and nonlinear categories were selected to form subsets with statistically similar mean evoked firing rates (pooled across all stimuli). The nonlinear subset still displays a higher number of bursts per stimulus. Black lines on bar graphs indicate 95% bootstrapped confidence intervals. D. Mean evoked spike rate is higher for nonlinear units than for linear, but with considerable

overlap between populations. Differences in bursting persist when subsets of units are matched for firing rates (see B, right panel).

Chapter 3

Development of Novel Bioluminescent Methods For Non-Invasive Optogenetic Control *In Vivo*

Author Contributions:

BTH designed in vivo experiments, performed viral injections, and collected and analyzed data. BTH assisted during slice recordings that were performed by Shane Crandall from Barry Connors' lab. Luminopsin constructs and data from cultured cells were provided by Ute Hochgeschwender. Some of these data were presented in the following publication:

Berglund K, Tung JK, **Higashikubo B**, et al. (2015) Combined Optogenetic and Chemogenetic Control of Neurons. In: Kianianmomeni A (ed) Optogenetics – Methods and Protocols. Springer New York (In Press)

Background

Control of Perceptual Information Relay by the Thalamic Reticular Nucleus

Incoming sensory information from all modalities, with the exception of olfaction, synapses in the thalamus on the way to neocortex. This sensory relay is uniquely positioned to act as a gate, to determine which inputs from the periphery are processed by the neocortex. A primary source of GABAergic control of thalamic relay nuclei that send information to neocortex is the thalamic reticular nucleus (TRN), a thin shell of neurons enveloping the thalamus. Projections from thalamocortical and corticothalamic cells synapse within this nucleus, and the TRN projects directly to the rest of thalamus, generating feedforward and feedback inhibition in this structure. The TRN is positioned to have a major influence on activity within the thalamocortical circuit, and its ability to drive bursting in relay nuclei and subsequent cortical oscillatory activity has been shown previously in our lab (Halassa et al., 2011).

Bursting: A Powerful Mode of Neural Activity in Health and Disease

A well-known property of thalamic projection neurons is their ability to fire action potentials in different modes, tonic or bursting, depending on the state of the network. A burst consists of multiple spikes fired in rapid succession (e.g., with an interval <4ms) preceded by periods of quiescence ≥100ms (Swadlow and Gusev, 2001). "Bursting" is a widely applied descriptor of neural activity, but in thalamic nuclei, this term specifically refers to a period of high frequency action potential firing mediated by a large underlying calcium event (a calcium "spike") (Crunelli et al., 1989; Huguenard and Prince, 1992; Coulon et al., 2009). *In vitro* studies have shown that many thalamic neurons (including thalamocortical projection cells and TRN cells) express T-type calcium channels that cause calcium spikes and bursts after a period of hyperpolarization. The TRN inhibits thalamocortical neurons, causing a hyperpolarization that de-inactivates T-channels. Upon release of inhibition, these channels are available to open, leading to a calcium spike with a burst of multiple concurrent sodium action potentials. The activity of these relay cells in turn provides an excitatory input to the TRN, forming an oscillatory loop. **The corollary of this biophysical reality is that sustained, weak depolarization in TRN neurons will *prevent* bursting in TRN neurons, by blocking the necessary hyperpolarization.**

The change from tonic to burst firing denotes a shift in thalamic network dynamics, but the role of bursting in information processing is debated. Some studies have argued that a burst is highly efficient at relaying information by virtue of the postsynaptic impact of several spikes fired in short succession (Swadlow and Gusev, 2001). In a contrasting view (Llinás and Steriade, 2006), bursting represents a state of inattention and impoverished signal relay. In support of this view, recent studies have shown that alpha rhythms—widely

believed to emerge from thalamic bursting at 5-15 Hz—occur in specific parts of sensory maps that are *disattended* in task performance (Worden et al., 2000; Foxe and Snyder, 2011). In either case—whether bursting is an optimal signal relay or the signature of a decreased probability of information relay—understanding any differences in the relative expression these events across thalamic nuclei will provide useful insight for leading theories of thalamocortical dynamics.

As stated previously, the rapid firing of multiple action potentials in a burst can be highly effective for driving activity in post-synaptic targets, potentially enhancing signal relay in the brain (Lesica, 2004; Alitto and Usrey, 2005; Lesica et al., 2006; Stanley, 2013). Excessive expression of this powerful activity pattern in thalamus is hypothesized to be causal in several diseases (Llinás et al., 1999). As a cardinal example, multiple types of epileptic seizures are believed to be driven by hyper-synchronized rhythmic bursting in the thalamic reticular nucleus (TRN) and in thalamic relay neurons that project to the neocortex (Beenhakker and Huguenard, 2009). The TRN is a shell of inhibitory neurons that target and hyperpolarize thalamic relay cells, generating rebound bursts. Epileptic seizures emerging from neocortical injury, and absence seizures, the most common form in children, are both believed to emerge from overly robust rates and synchrony of thalamic bursting (Avanzini et al., 1996; Beenhakker and Huguenard, 2009; Paz et al., 2013). Thalamic burst-driven seizure activity is hypothesized to be an altered form of endogenous patterns observed in slow-wave sleep called *spindles*, bouts of rhythmic thalamic bursting typically lasting ~0.5-1.5 seconds (Kostopoulos, 2000; Beenhakker and Huguenard, 2009).

Decreased rhythmic thalamic bursting is also implicated in several diseases. Schizophrenic patients show lower spindles rates and lower coherence in spindle expression across neocortex. These changes directly predict memory impairment and positive symptoms (Ferrarelli et al., 2007; 2010). Recent advances are beginning to allow direct causal control of burst and spindle dynamics *in vivo*: Our lab has recently demonstrated, using *in vivo* chronic multi-electrode recording in freely behaving mice, that direct *transient* optogenetic driven depolarization of TRN enhances burst probability and triggers spindles (Halassa et al., 2011). We have extended this work by characterizing the responses of TRN neurons to 'traditional' optogenetic drive *in vivo*, using the VGAT-ChR2 mouse model. This transgenic animal expresses Channelrhodopsin-2 under the control of the vesicular GABA transporter—therefore the inhibitory TRN has high expression of ChR2, while somatosensory relay nuclei are unaffected. This preparation allows for selective targeting of TRN neurons by careful fiber positioning and monitoring of light output. These experiments showed heterogeneity across TRN cells with regard to stimulus response properties, but also found a clear relationship between the strength of optical drive and the bursting behavior of the TRN both in single neurons and in the activity of the larger circuit. Specifically, long-duration stimulation of TRN reliably drives bursts in targeted units and triggers spindle-like bouts of rhythmic activity (see Chapter 2). **Figure 1** shows the probability of spindle-frequency bursting as a function of stimulus duration, as determined using a hierarchical Bayesian model (black lines indicate 95% highest density intervals). These conclusions, based on multi-unit recordings, were derived from 15 sessions of stimulation across 60 electrodes.

Similar trends were seen at the level of single units, with optogenetic drive reliably evoking burst firing in TRN cells, both directly and for several hundred milliseconds following stimulus offset. **Figure 2** shows 600 trials of optogenetic stimulation in a single unit, with each spike indicated by a gray dot, and each burst indicated by colored points. On almost all trials, optogenetic drive at time zero drove an immediately following burst. Enhanced bursting was also observed >150 milliseconds later. In total, over 100 well-isolated single units were recorded from seven mice using silicon laminar probes customized for optogenetic drive: In 15%, enhanced bursting was observed following the longest transient depolarization, as opposed to <2% following a 5ms stimulus.

This characterization of TRN burst dynamics driven by *transient* depolarization provides a foundation from which to pursue a novel, minimally invasive approach to the regulation of thalamic activity that is described below. Specifically, I will in subsequent studies use a novel means of inducing sustained, weak depolarization to test the hypothesis that this kind of "DC" manipulation *decreases* the probability of burst production by preventing necessary hyperpolarization.

BL-OG: Burst Regulation in Single Neurons by Integrating Bioluminescence with Optogenetics

Here, I describe a novel approach for burst regulation. This approach leverages bioluminescence (BL). In BL reactions, photons are produced when an enzyme (a *luciferase*) binds a co-factor (a *luciferin*) (Ohmiya and Hirano, 1996; Sato et al., 2004). When central neurons express luciferase *in vivo,* they emit brightly after peripheral luciferin

injection, as luciferins can cross cell membranes and the blood-brain barrier (Shah et al., 2008; Kauer et al., 2012; Li et al., 2013). **Figure 3** shows an example in which neocortical neurons in the right hemisphere were transduced with a BL enzyme (Gaussia luciferase) by viral transduction. After intravenous injection of the appropriate luciferin (Coelenterazine, CTZ), these cells emitted brightly, allowing localization of the BL generator through the scalp using an IVIS imaging system (pseudocolored region). This form of "cold light" is already widely used in longitudinal *in vivo* studies, and is safe for chronic use in the brain (Deroose et al., 2006; Tiffen et al., 2010).

The strategy of using BL to drive optogenetics (BL-OG) was recently developed in our lab and by our close collaborator Dr. Ute Hochgeschwender, and has been vetted in neocortical neurons (Berglund et al., 2013; 2016). A key innovation has been development of *Luminopsins*, fusion proteins tethering BL sources to optogenetic receivers by a 15 amino acid linker. **Figure 4A** shows the efficacy in cultured neocortical neurons of the most recent Luminopsin (LMO3), which employs a bright BL source: enhanced Gaussia luciferase (**Figure 5**). When CTZ is presented, light production drives an immediate increase in action potential firing (**Figure 4A**). When the same BL emitter was tethered to a hyperpolarizing optogenetic element (Arch) and expressed in a different neuron, spontaneous firing was suppressed with CTZ presentation (**Figure 4B**).

The use of bioluminescence to modulate brain activity holds great promise for both basic research and future translational applications. The ability to drive optogenetic proteins by chemical means allows the technique to inherit many of the advantages of chemogenetic

approaches while utilizing the ongoing development of new opsins. General properties of BL-OG as utilized in this study are as follows:

1. BL-OG allows for the activation of well-characterized optogenetic proteins without the need for implanted fiber optics or major surgery.
2. This technique can benefit from presently known and newly developed optogenetic sensors and bioluminescent emitters, allowing for a number of response properties and potentially multiple effectors within the same system.
3. BL-OG is optimal for modulation on multiple timescales, as the route of luciferin administration and the temporal characteristics of the opsin can be combined o drive effects from seconds to many minutes.
4. BL-OG can be used to simultaneously modulate the activity of cells spread throughout the body. Luciferins can be administered systemically, so the potential distribution of light is limited only by the distribution of luciferases, rather than by the properties of the illumination system.
5. Because the light emitter is a protein, BL-OG can be directed to specific cells and/or cellular compartments. This provides a means for highly focused modulation to be controlled by an organism-wide intervention (i.e. systemic injection of substrate), while providing an opportunity for more complex paradigms involving multiple, independently-targeted effectors.

A key feature of this method is the ability to generate photons of a desired wavelength without the need for invasive implanted devices. Light delivery is a major consideration in

any use of optogenetics *in vivo*, as stimulating cells below the cortical surface requires tissue penetration. The extent of photon propagation through the brain is limited by light scattering and absorption, which is especially pronounced at shorter wavelengths (such as the blue light used to excite ChR2) (Aravanis et al., 2007). These effects are then combined with the simple geometric falloff of intensity from a point source. Increasing the power of the light source can activate larger volumes of brain tissue, but this must be kept in check to avoid tissue damage via heating. In addition to engineering challenges, any chronic implant causes damage to nearby cells and over time will lead to gliosis. The advantages of an entirely biological means of light production are extremely relevant for the modulation of the TRN, as its subcortical location and irregular shape present difficulties for even stimulation. A major goal of our *in vivo* experiments was to modulate firing properties of TRN neurons for an extended time, so the level of temporal control of BL-OG was well-suited for this purpose; the millisecond precision of a traditional laser or LED source was unnecessary for proof of concept data.

Materials and methods

Slice preparation

Slice data was recorded in collaboration with Shane Crandall from the Connors lab. LMO3 was expressed in the thalamus of two juvenile WT mice 7-12 days prior to recording. Whole cell patch recordings were done in thalamocortical slices while 100μM CTZ was infused into the recording chamber.

In vivo

Nine adult wild type (C57BL/6) mice were injected in TRN according to stereotaxic coordinates with an AAV construct consisting of LMO3 with an eYFP tag. A craniotomy was made at approximate coordinates 1.9mm lateral and 1.7mm posterior to bregma, and 0.7μl of virus was injected at a depth of 3mm using a pulled glass pipette.

Two to four weeks post-injection, recordings were performed under light (0.9%-1.1%) isoflurane anesthesia using 16 channel laminar silicon probes (Neuronexus). In all mice, baseline TRN activity was recorded for 10-15 minutes prior to injection of CTZ. CTZ was prepared as a 3.33mg/ml solution using the 'Fuel-Inject' solvent from Nanolight, and was injected either IV (tail vein) or IP to provide 250μg CTZ per animal. As the expected timing and intensity of the bioluminescence reaction depends on the route of CTZ administration (Aswendt 2013 plos), recordings were continued for up to ~1 hour following injection.

Results

Superfusion of CTZ in slice causes depolarization of LMO3-expressing neurons

eYFP reporter fluorescence in thalamocortical sections showed a strong bias to TRN as opposed to VB in our LMO3 expression (**Figure 6A**). The TRN was not specifically targeted in these mice, and this appears to be a function of our virus – the AAV 2/9-hSyn-LMO3 used in these experiments shows tropism for inhibitory cells in our experience.

LMO3 expressing cells were electrophysiologically normal in response to current injection, showing tonic firing after depolarization and rebound bursts following prolonged hyperpolarization (**Figure 6B**). Expressing cells also behaved as expected when stimulated

with blue light, demonstrating that VChR1 functions normally when incorporated into the fusion protein (**Figure 6C**).

Neurons were recorded in voltage clamp mode (n=3 cells, two animals) during application of CTZ to determine the effect on membrane potential. With the level of expression in these slices, 100μM CTZ led to 1-3mV of reversible depolarization. Because bursting in TRN cells is reliant on the deinactivation of T-type calcium channels by hyperpolarization, we characterized induced bursts in the presence of CTZ. The level of depolarization observed was not sufficient to prevent infected TRN cells from bursting, but delayed the onset of evoked bursts (**Figure 6E-F**). Given the potential for increased expression levels or enhanced photocurrents in future iterations of luminopsins, these data suggest that BL-OG could be used for the modulation of timing or probability of T-current driven bursting.

Injected CTZ drives increased spiking in LMO3-infected TRN *in vivo*

Systemic administration of CTZ via IV or IP injection led to an increase in spike rate, the timing of which corresponded to the expected availability of the luciferin given the different routes of administration. Multiunit recordings from TRN during IP injections showed a small increase in firing over a period of tens of minutes (**Figure 7**), in some cases lasting 40+ minutes from the time of CTZ administration. Figure 7 shows averaged MUA from four LMO3-infected mice and four controls after CTZ injection. Increased mean firing persisted for ~11 minutes before returning to baseline in the LMO3 cohort. Interestingly, spiking in controls was elevated for 1-1.5 minutes after CTZ injection, but with significantly lower amplitude than the LMO3 animals. Further testing is necessary to determine whether

this is a direct effect of CTZ or its solvent on TRN activity, or whether it reflects the somatosensory response to the injection itself. Due to the low peak activity of bioluminescence after IP injection, single unit activity was not reliable during these trials.

During IV injections of CTZ, MUA and sorted single units from TRN showed reliable, short-lasting modulation of firing rate. Onset of this increase occurred within seconds of injection, peaking at around 20s after the injection was completed (**Figure 8**). Activity declined with a slower time constant, returning to baseline after ~2 minutes. In one animal, two IV trials were conducted during the same recording and displayed similar temporal characteristics as well as similar amplitude of modulation in the MUA.

Single unit recordings also revealed preliminary evidence for modulation of bursting in VB after IV injection of CTZ. In one recording (**Figure 8**), a putative VB relay cell was recorded simultaneously with TRN units (as determined by spike waveform shape and localization of the unit on the electrode shank). This unit responded in an opposite direction to the MUA and other single units, with a firing rate that decreased from baseline after CTZ injection. The timing of this change in activity matched that for the increases in other cells, and an increase in burst rate was seen at the local minimum of spike rate. We hypothesize that this phenomenon was the result of LMO3-mediated stimulation of TRN units driving inhibition of downstream relay nuclei. Hyperpolarization generated by GABAergic input from throughout the expression zone in TRN could de-inactivate T-type calcium channels in VB, thus increasing the likelihood of burst vs. tonic firing.

Conclusions

While the data described are preliminary, they provide proof of concept for the use of BL-OG in multiple brain structures in slice and in vivo. The luminopsin used in these experiments was the third iteration of a fusion protein based on a natural bioluminescent emitter and an excitatory opsin, which has proven to have biologically relevant effects in the intact brain. Further experimentation will be necessary to characterize the degree of variability in this preparation, as well as its long-term stability. The relatively low *n* of this study reflects the degree to which this entire approach is still in development, and there are a number of routes for optimizing *in vivo* effectiveness.

The effect of CTZ on firing rate is dependent on a number of factors that are open to experimental control but not fully determined in the current data set. An obvious determinant for any virally transduced protein is the level and consistency of viral expression in the tissue. These preliminary experiments only used extracellular recording as the readout of activity, so it was not possible to correlate the behavior of a single cell or of a region with the amount of LMO3 (measured by reporter expression) or the strength of bioluminescence (which would require a high sensitivity camera or photomultiplier tube). Experiments going forward will incorporate EMCCD cameras in order to provide simultaneous measurement of light emission over time.

A possible concern moving forward with these techniques *in vivo* is the determination of availability of the luciferase substrate. Systemic delivery of a luciferin has many advantages over direct delivery to the area of interest, but comes at the expense of precise spatial and

temporal control. The expected amount of luminescence from an IP injection is low, making detection of modulation difficult in single trials with significant background fluctuations, but the slow timecourse poses difficulties for doing multiple trials within an acute recording session. Moving to a chronically implanted mouse preparation would allow for more recordings over time. By contrast, IV injections are fast acting and deliver a much higher peak concentration of CTZ to the bloodstream than IP. The small volume of liquid that can be safely administered to a mouse via this route leaves room for high variability between injections, however.

New protein constructs are under active development, and the general technique of combined bioluminescence and optogenetics can be extended in a variety of ways. Obvious future directions include the use of inhibitory optogenetic effectors (such as proton pumps or chloride channels) to allow for suppression or silencing of activity in response to the appropriate luciferin (Tung et al., 2015). The diversity of naturally occurring and modified luciferases provides the possibility of using opsins sensitive to a range of excitation wavelengths – in theory this approach could be used for bidirectional control of activity in single cells, or selective non-invasive modulation of distinct cell populations.

References

Alitto HJ, Usrey WM. Dynamic properties of thalamic neurons for vision. *Prog Brain Res* 149: 83–90, 2005.

Aravanis AM, Wang L-P, Zhang F, Meltzer LA, Mogri MZ, Schneider MB, Deisseroth K. An optical neural interface: in vivo control of rodent motor cortex with integrated fiberoptic and optogenetic technology. *J Neural Eng* 4: S143–56, 2007.

Avanzini G, de Curtis M, Franceschetti S, Sancini G, Spreafico R. Cortical versus thalamic mechanisms underlying spike and wave discharges in CAERS. *Epilepsy Res* 26: 37–44, 1996.

Beenhakker MP, Huguenard JR. Neurons that fire together also conspire together: is normal sleep circuitry hijacked to generate epilepsy? *Neuron* 62: 612–632, 2009.

Berglund K, Birkner E, Augustine GJ, Hochgeschwender U. Light-emitting channelrhodopsins for combined optogenetic and chemical-genetic control of neurons. *PLoS ONE* 8: e59759, 2013.

Berglund K, Tung JK, Higashikubo B, Gross RE, Moore CI, Hochgeschwender U. Combined Optogenetic and Chemogenetic Control of Neurons. *Methods Mol Biol* 1408: 207–225, 2016.

Coulon P, Herr D, Kanyshkova T, Meuth P, Budde T, Pape H-C. Burst discharges in neurons of the thalamic reticular nucleus are shaped by calcium-induced calcium release. *Cell Calcium* 46: 333–346, 2009.

Crunelli V, Lightowler S, Pollard CE. A T-type Ca2+ current underlies low-threshold Ca2+ potentials in cells of the cat and rat lateral geniculate nucleus. *J Physiol (Lond)* 413: 543–561, 1989.

Deroose CM, Reumers V, Gijsbers R, Bormans G, Debyser Z, Mortelmans L, Baekelandt V. Noninvasive monitoring of long-term lentiviral vector-mediated gene expression in rodent brain with bioluminescence imaging. *Mol Ther* 14: 423–431, 2006.

Ferrarelli F, Huber R, Peterson MJ, Massimini M, Murphy M, Riedner BA, Watson A, Bria P, Tononi G. Reduced sleep spindle activity in schizophrenia patients. *Am J Psychiatry* 164: 483–492, 2007.

Ferrarelli F, Peterson MJ, Sarasso S, Riedner BA, Murphy MJ, Benca RM, Bria P, Kalin NH, Tononi G. Thalamic dysfunction in schizophrenia suggested by whole-night deficits in slow and fast spindles. *Am J Psychiatry* 167: 1339–1348, 2010.

Foxe JJ, Snyder AC. The Role of Alpha-Band Brain Oscillations as a Sensory Suppression Mechanism during Selective Attention. *Front Psychol* 2: 154, 2011.

Halassa MM, Siegle JH, Ritt JT, Ting JT, Feng G, Moore CI. Selective optical drive of

thalamic reticular nucleus generates thalamic bursts and cortical spindles. *Nat Neurosci* (July 24, 2011). doi: 10.1038/nn.2880.

Huguenard JR, Prince DA. A novel T-type current underlies prolonged Ca(2+)-dependent burst firing in GABAergic neurons of rat thalamic reticular nucleus. *Journal of Neuroscience* 12: 3804–3817, 1992.

Kauer TM, Figueiredo JL, Hingtgen S, Shah K. Encapsulated therapeutic stem cells implanted in the tumor resection cavity induce cell death in gliomas. *Nat Neurosci* 15: 197–204, 2012.

Kostopoulos GK. Spike-and-wave discharges of absence seizures as a transformation of sleep spindles: the continuing development of a hypothesis. *Clin Neurophysiol* 111 Suppl 2: S27–38, 2000.

Lesica NA, Weng C, Jin J, Yeh C-I, Alonso J-M, Stanley GB. Dynamic Encoding of Natural Luminance Sequences by LGN Bursts. *PLoS Biol* 4: e209, 2006.

Lesica NA. Encoding of Natural Scene Movies by Tonic and Burst Spikes in the Lateral Geniculate Nucleus. *J Neurosci* 24: 10731–10740, 2004.

Li X-F, Deng Y-Q, Zhao H, Ye Q, Wang H-J, Li S-H, Zhu S-Y, Shi P-Y, Qin E-D, Zhang B, Qin C-F. Noninvasive bioluminescence imaging of dengue virus infection in the brain of A129 mice. *Appl Microbiol Biotechnol* 97: 4589–4596, 2013.

Llinás RR, Ribary U, Jeanmonod D, Kronberg E, Mitra PP. Thalamocortical dysrhythmia: A neurological and neuropsychiatric syndrome characterized by magnetoencephalography. *Proc Natl Acad Sci USA* 96: 15222–15227, 1999.

Llinás RR, Steriade M. Bursting of thalamic neurons and states of vigilance. *J Neurophysiol* 95: 3297–3308, 2006.

Ohmiya Y, Hirano T. Shining the light: the mechanism of the bioluminescence reaction of calcium-binding photoproteins. *Chem Biol* 3: 337–347, 1996.

Paz JT, Davidson TJ, Frechette ES, Delord B, Parada I, Peng K, Deisseroth K, Huguenard JR. Closed-loop optogenetic control of thalamus as a tool for interrupting seizures after cortical injury. *Nat Neurosci* 16: 64–70, 2013.

Sato A, Klaunberg B, Tolwani R. In vivo bioluminescence imaging. *Comp Med* 54: 631–634, 2004.

Shah K, Hingtgen S, Kasmieh R, Figueiredo JL, Garcia-Garcia E, Martinez-Serrano A, Breakefield X, Weissleder R. Bimodal viral vectors and in vivo imaging reveal the fate of human neural stem cells in experimental glioma model. *J Neurosci* 28: 4406–4413, 2008.

Stanley GB. Reading and writing the neural code. *Nat Neurosci* 16: 259–263, 2013.

Swadlow HA, Gusev AG. The impact of "bursting" thalamic impulses at a neocortical synapse. *Nat Neurosci* 4: 402–408, 2001.

Tiffen JC, Bailey CG, Ng C, Rasko JEJ, Holst J. Luciferase expression and bioluminescence does not affect tumor cell growth in vitro or in vivo. *Mol Cancer* 9: 299, 2010.

Tung JK, Gutekunst C-A, Gross RE. Inhibitory luminopsins: genetically-encoded bioluminescent opsins for versatile, scalable, and hardware-independent optogenetic inhibition. *Sci Rep* 5: 14366, 2015.

Worden MS, Foxe JJ, Wang N, Simpson GV. Anticipatory biasing of visuospatial attention indexed by retinotopically specific alpha-band electroencephalography increases over occipital cortex. *J Neurosci* 20: RC63, 2000.

Figures

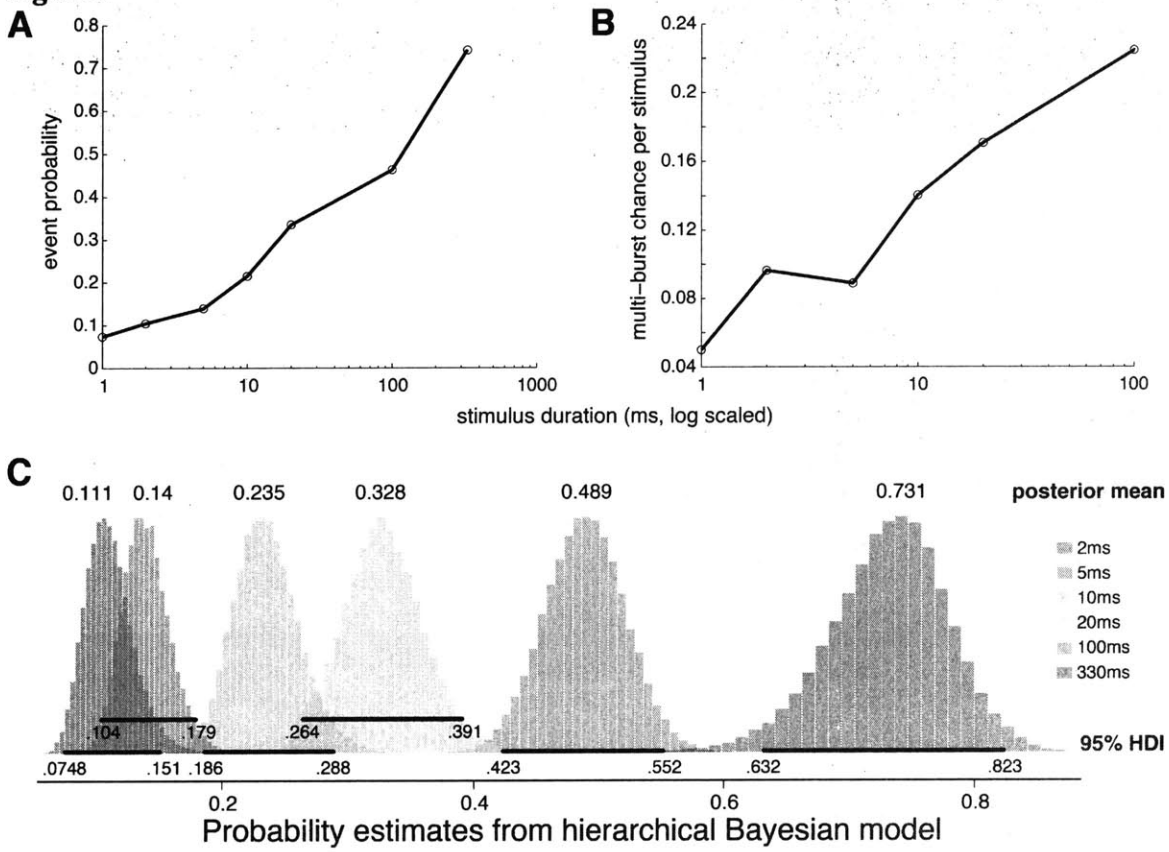

Figure 1

A-B. Frequency of MUA 'bursts' and the number of events per stimulus increases proportionally to stimulus duration. All pairwise comparisons of event frequency are significant at the $p<.05$ level. C. Hierarchical model of data from (A) provides confidence bounds on estimates while adjusting certainty for sample size. Model treats event occurrence as a binomial process with the event probability for any given channel drawn from a higher-level distribution at each stimulus duration. Each color represents the modeled posterior distribution for event frequency at a given stimulus duration.

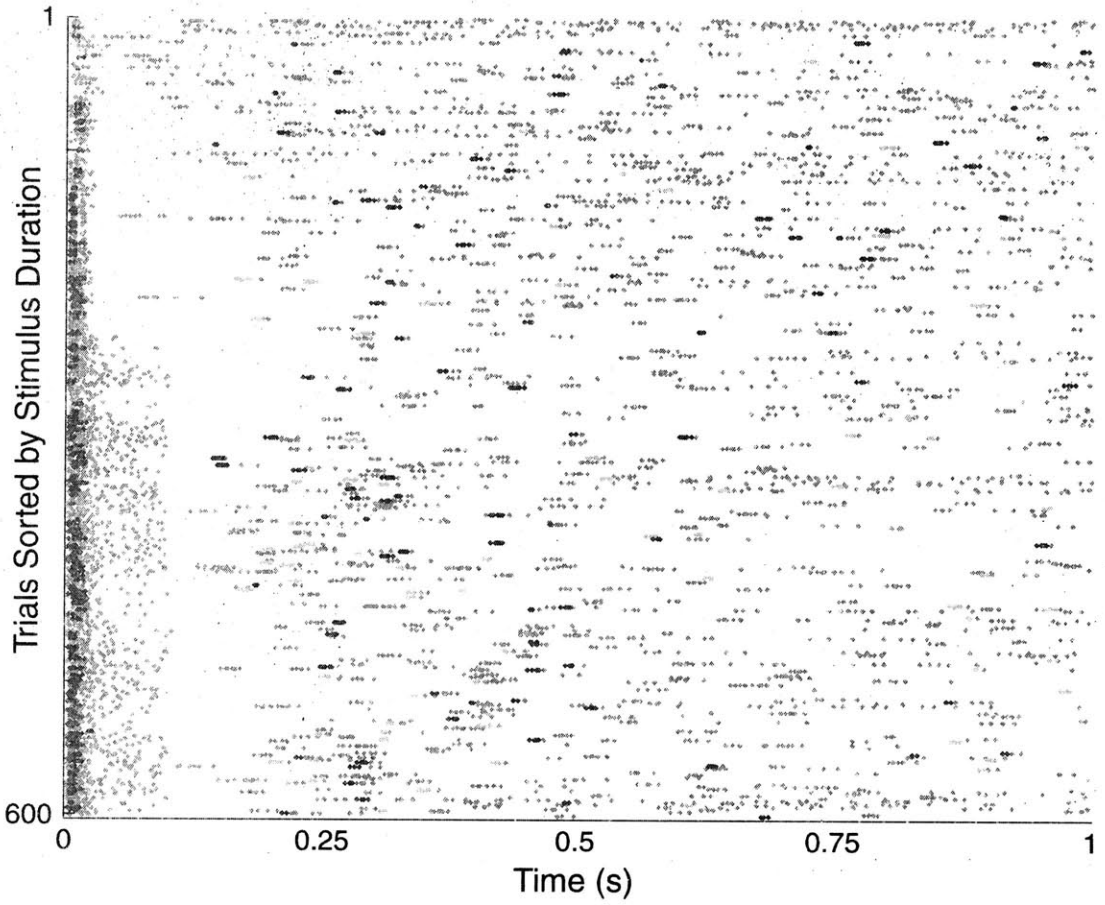

Figure 2

Extracted bursts from one example sorted unit in a given session are shown, with responses ordered by stimulus duration from *top* (shortest, 2 milliseconds duration) to *bottom* (longest, 100 milliseconds duration). Bursts were classified as spikes with a 4ms or less inter-spike interval, preceded by at least 100ms of silence (see Methods for details). *Gray dots* indicate single spikes. *Dark blue dots* indicate the first extracted burst for a given stimulus (many occurring during the stimulation period). Other colors indicate bursts occurring after light cessation: *Green* second burst; *Orange* third burst.

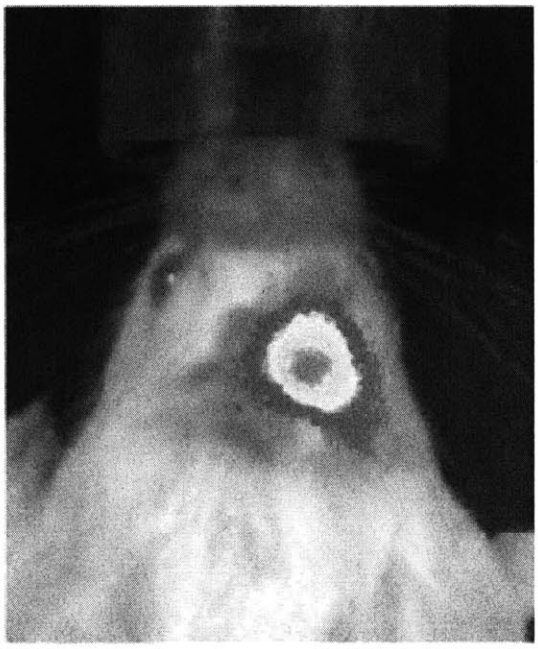

Figure 3

Bioluminescence can be driven *in vivo* following intravenous delivery of luciferins. In this example, Gaussia luciferase was expressed in cortical cells of the right hemisphere using viral transduction. Colored region shows light emission after injection of CTZ, as measured by an EMCCD camera system.

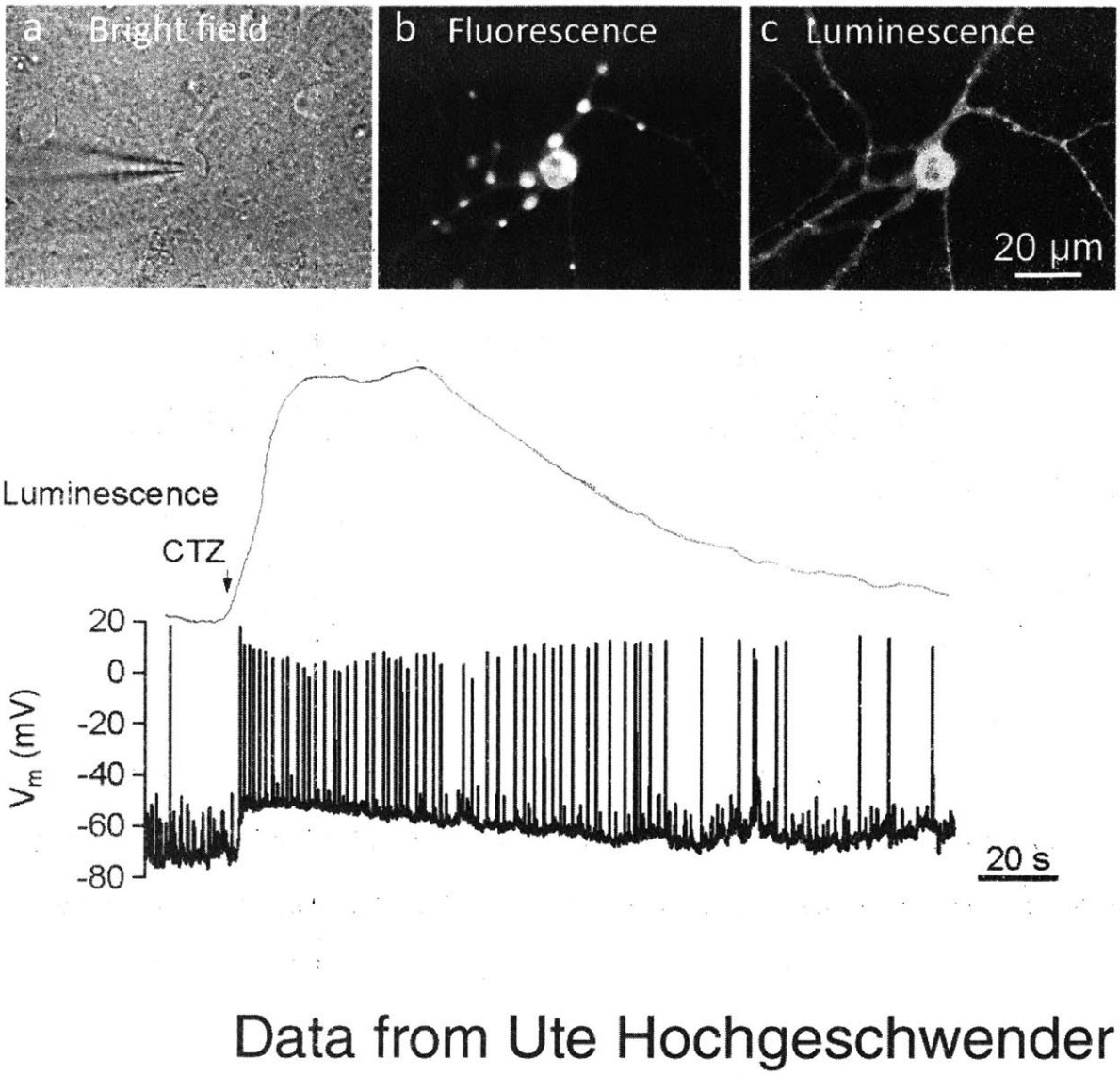

Figure 4

LMO3 is active in cultured neurons. Cells expressing LMO3 were recorded during bath application of CTZ with simultaneous measurements of bioluminescence. CTZ application led to a rapid increase in brightness followed by membrane depolarization and spiking. The effects of LMO3 on Vm fall off in time with the decrease in light production.

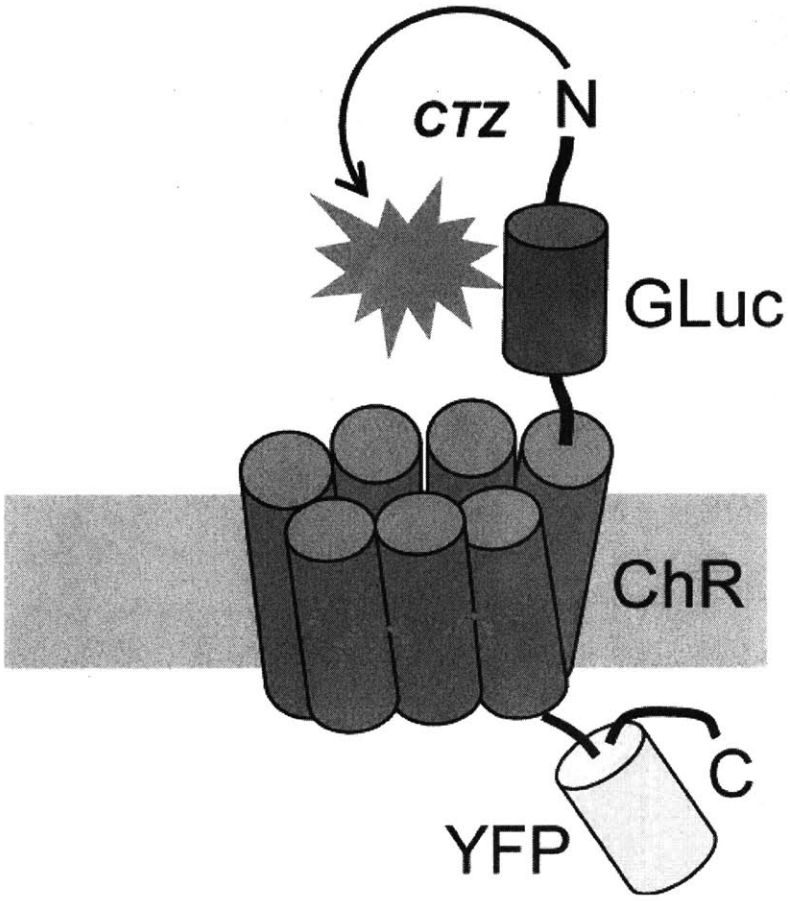

Figure 5

Structure of LMO3: light is produced by the oxidation of CTZ by Gaussia luciferase tethered to Volvox channelrhodopsin. See text for details.

Figure 6

Slice recordings courtesy of Shane Crandall

LMO3 expressed in TRN cells does not change normal dynamics, but confers sensitivity to CTZ. See text for experimental details.

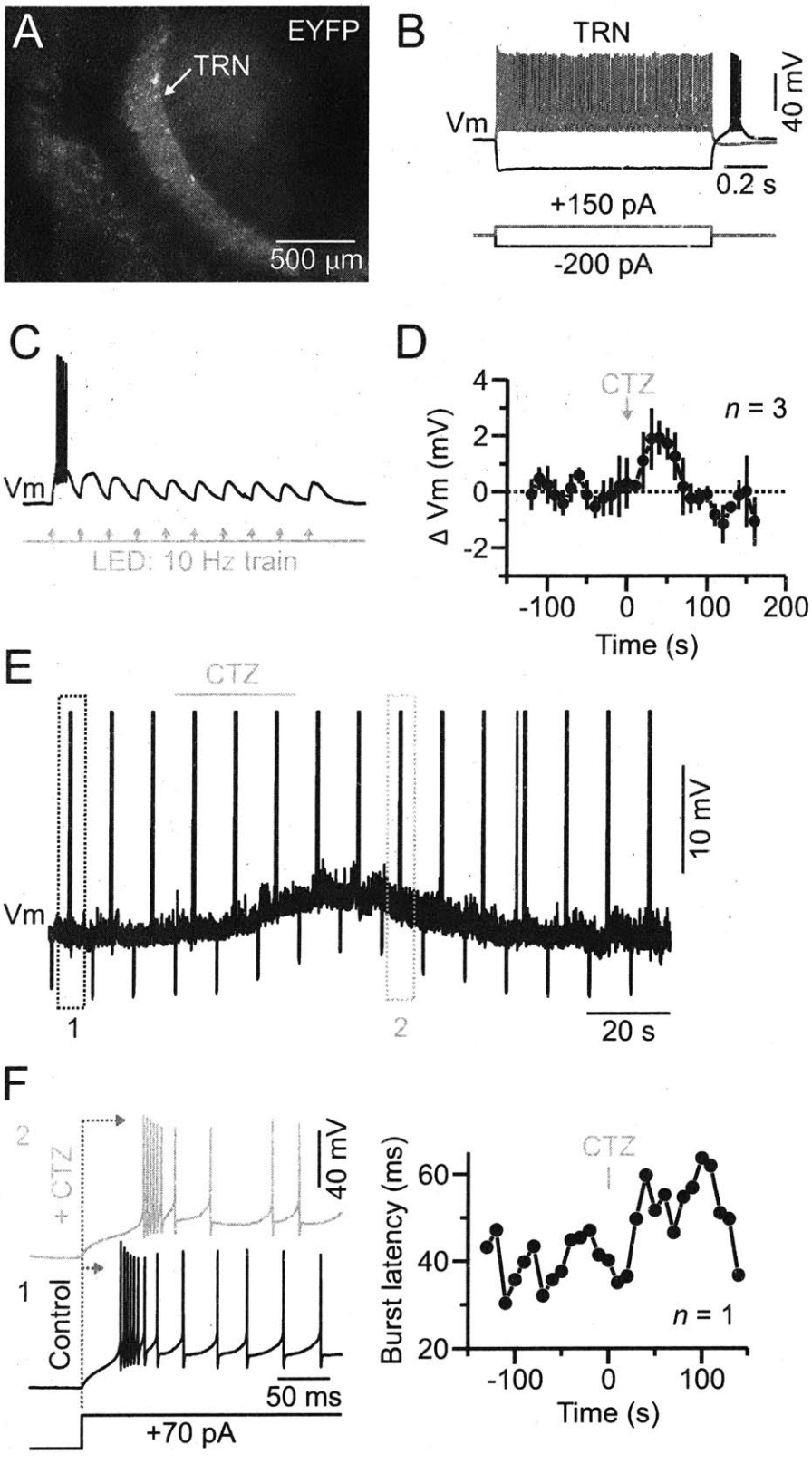

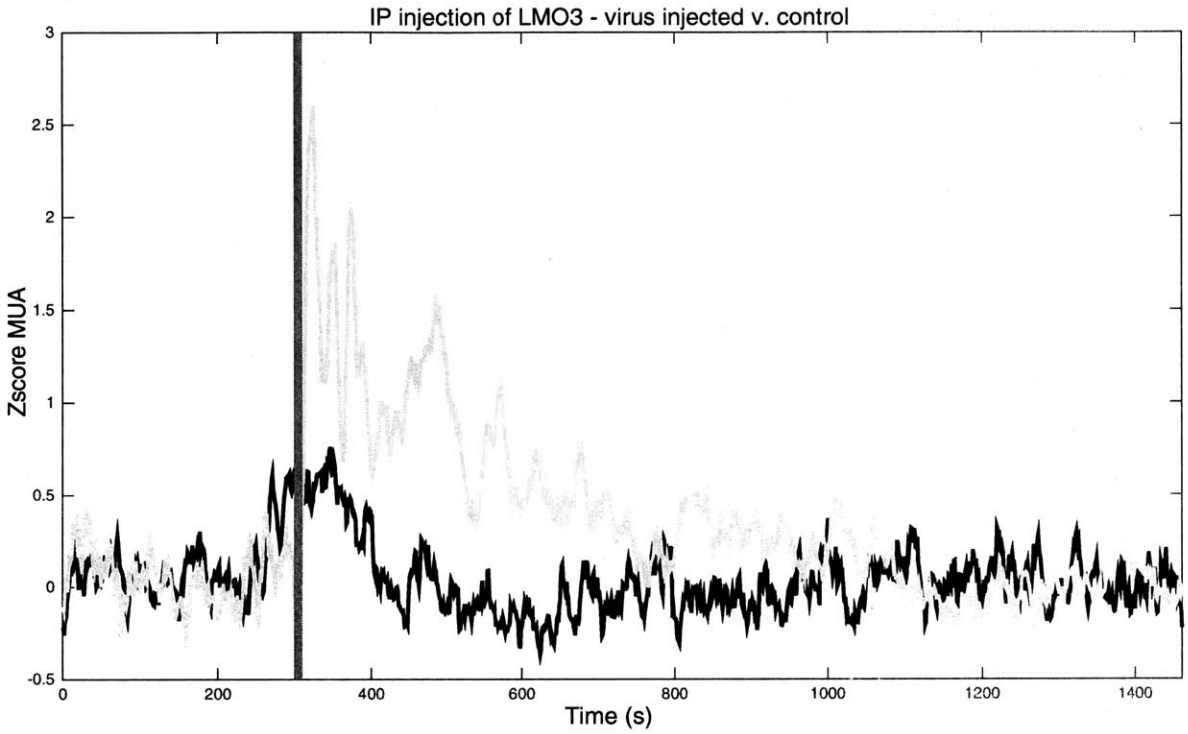

Figure 7

Red line indicates time of intraperitoneal CTZ injection. Experimental animals were injected in TRN with an AAV containing the LMO3 construct 2-4 weeks prior to recording. N=4 mice expressing LMO3, n = 4 control animals

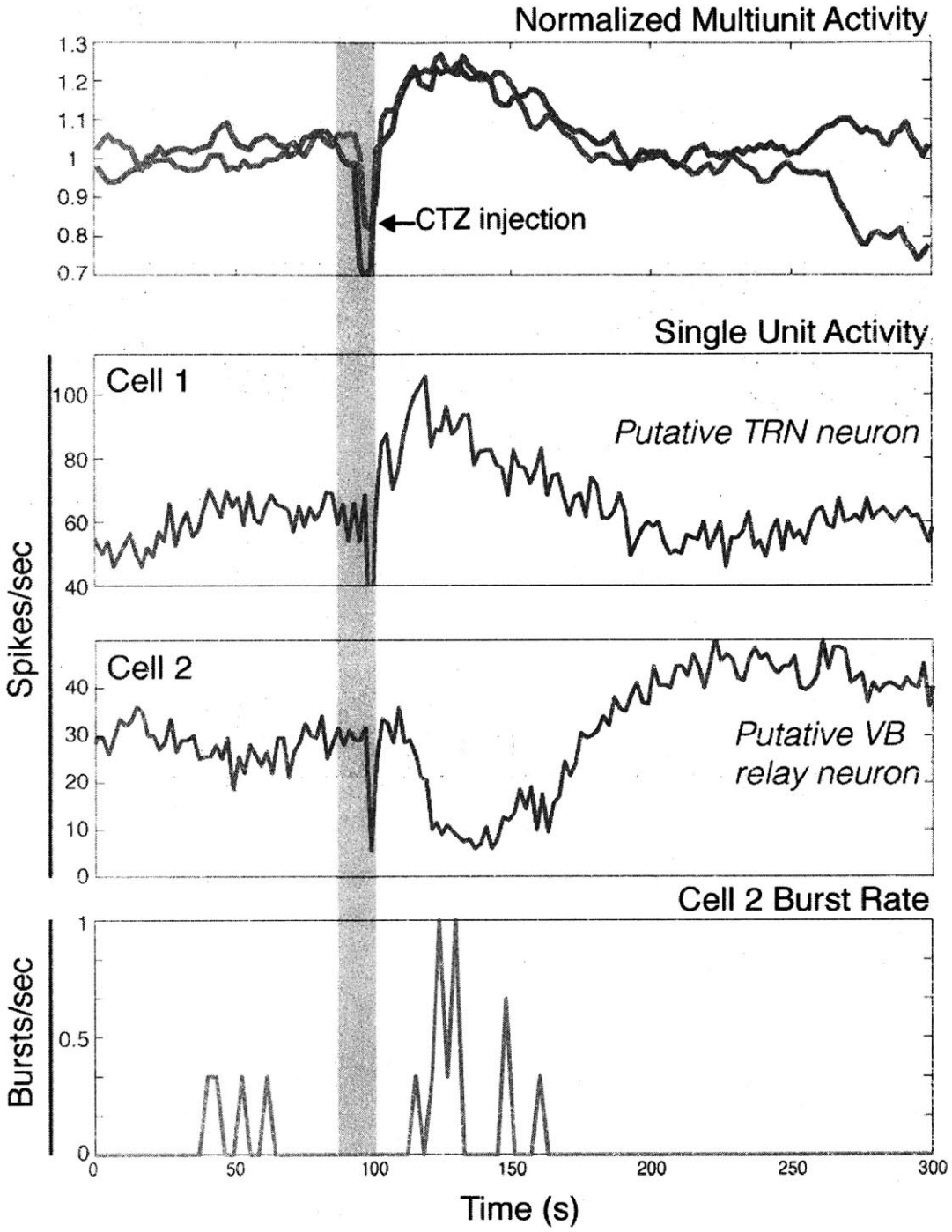

Figure 8

Multi-unit and single unit recordings following IV injection of CTZ in an LMO3 expressing mouse. Traces in top panel are from injections separated by ~15 minutes.

Chapter 4

Conclusions

Future experiments:

1. Targeted projections from first and second order sensory nuclei in the TRN.

Data from Chapter 2 provided clear physiological evidence for heterogeneous evoked activity within a small region of the TRN. Because the TRN is composed of entirely inhibitory neurons it has sometimes been viewed as a monolithic structure, but data from cell traces, protein expression, and subdivision by projection pattern now suggest that the TRN could support a great deal of functional heterogeneity (Clemence and Mitrofanis, 1992; Deschênes et al., 1996; Pinault and Deschênes, 1998a; 1998b; Desîlets-Roy et al., 2002; Halassa et al., 2014). We found distinct firing patterns between two groups of cells in a preparation much reduced from the complexity of inputs associated with naturalistic behavior. While anesthesia likely affected the baseline activity and excitability of thalamic neurons, our objective was to eliminate some of the variability that would naturally be associated with changes in arousal or from ongoing sensory input. Our stimulus parameters were designed to be temporally simple and well above threshold, but there was still space for interesting nonlinearities to arise. These experiments and the work on TRN heterogeneity from other groups suggest some clear next steps for determining possible substrates underlying our observed subpopulations.

Anatomical studies from Pinault, Deschenes and colleagues provided motivation early on to look for variability in the activity of cells in somatosensory regions of TRN. Targeting particular projections *in vivo* is now possible using viral techniques such as those employed by Halassa et al. (2014) to distinguish between sensory and limbic-projecting neurons. One approach to build on both bodies of work would be to use retrograde viral transduction to

target projections to more similar thalamic nuclei. In the context of the rodent somatosensory system, a primary relay nucleus (VPm) and a higher-order sensory nucleus (POm) could be targeted with ChR2 to allow direct stimulation of morphologically distinct subsets of cells. With the right combination of wavelength-shifted opsins and careful stereotaxic injections, it may be possible to target both populations in the same animal, providing better within-experiment consistency while allowing optogenetically tagged cells to be recorded in response to stimulation of the other subgroup. Given the existence of intra-TRN synaptic connections and open feedback loops with regions of thalamus and cortex, this could reveal the presence (or absence) of cross-group connectivity. An additional possibility with this approach would be to investigate the laminated structure of somatosensory TRN directly in the intact brain. Given the thin shell-like shape of the TRN, dense laminar electrode arrays could span its entire thickness, simultaneously recording from cells with different projection patterns.

2. SOM vs. PV functional characterization

Another distinction within TRN cells that has not been functionally characterized is the activity patterns of PV vs. SOM expressing neurons. On the gross level, both are expressed widely throughout the extent of the structure (Graybiel and Elde, 1983; Oertel et al., 1983; Sun et al., 2002; Albéri et al., 2013; Ahrens et al., 2015), but not all cells express both. In the mouse, these populations can be targeted using recombination systems and viruses--by crossing already available mouse lines (for example PV-Flp with SOM-Cre), it may be possible to separately target these groups within the same animal. Opsins that can be

targeted without overlap would provide the means to separate these populations while recording *in vivo*, while more detailed characterization on the single cell level would be straightforward in slice. There is evidence for PV involvement in shaping the burst properties of TRN cells, and for SOM in the regulation of oscillations (Sun et al., 2002; Albéri et al., 2013), so the interaction between these effects could shape the most fundamental properties of the thalamocortical circuit.

3. LMOs for regulation of epileptic seizures.

In Chapter 3 we described progress in developing BL-OG, a system of techniques that use bioluminescence as an excitation source for optogenetics. While many aspects of this approach are still being developed, validation of its effectiveness *in vivo* opens the door for many experiments using the current generation of tools. In the TRN, normal and abnormal rhythmicity are areas of great interest clinically. Absence seizures are believed to originate in rhythmic burst activity that resonates between the TRN and relay nuclei. Bursting in thalamic cells is dependent on membrane potential, so subtle shifts in Vm over long periods of time could be driven via BL-OG to regulate burst rate on behaviorally relevant timescales. Traditional optogenetics has been used to interrupt seizures by targeting the TRN (Paz et al., 2013), so a first step for testing the efficacy of BL-OG in this context would be to transduce LMOs into the TRN of a mouse model with spontaneous seizures. Behavioral monitoring combined with chronic recording in freely behaving animals could be used to compare seizure rates with or without the luciferase substrate, while correlating behavioral output with burst firing.

The success of this approach depends largely on the strength/duration of modulation by LMOs and the availability of luciferin. Our preliminary data are mixed with regard to the applicability of LMO3 in this context: in slice preparations the amount of depolarization was sufficient to delay bursts, but not to abolish induced burst activity. In spite of this, our *in vivo* results showed modulation of spike rate, suggesting a significantly larger effect. This could be due to a number of factors: for technical reasons all slice experiments were performed using young mice and approximately 2 weeks of expression time for the virus, while *in vivo* mice were injected as adults and were given up to 4 weeks of incubation time. It is also possible that the effect seen *in vivo* requires a level of aggregate activity that is more readily obtained with the connections present in an intact brain. Fortunately, both the timing and strength of luminopsin effects have potential for modification. At the level of the emitter, there are a wide variety of available luciferases and substrates to choose from. On a basic level, molecular engineering of luciferin variants can be used to change the kinetics of the bioluminescent reaction. The affinity of the luciferin to the luciferase enzyme, the total photon flux, and the timing of light production ('flash' vs 'glow) are all affected by modification of the substrate. On the receiver side, there has been an explosion of optogenetic tools in recent years, and different luciferase-opsin combinations are being tested for their efficacy in neurons. For long-term activation or suppression of cells, step-function opsins are especially promising as a simple way to increase the duration of a BL-OG effect for any given reaction.

References

Ahrens S, Jaramillo S, Yu K, Ghosh S, Hwang G-R, Paik R, Lai C, He M, Huang ZJ, Li B. ErbB4 regulation of a thalamic reticular nucleus circuit for sensory selection. *Nat Neurosci* 18: 104–111, 2015.

Albéri L, Lintas A, Kretz R, Schwaller B, Villa AEP. The calcium-binding protein parvalbumin modulates the firing 1 properties of the reticular thalamic nucleus bursting neurons. *J Neurophysiol* 109: 2827–2841, 2013.

Clemence AE, Mitrofanis J. Cytoarchitectonic heterogeneities in the thalamic reticular nucleus of cats and ferrets. *J Comp Neurol* 322: 167–180, 1992.

Deschênes M, BOURASSA J, Doan VD, Parent A. A single-cell study of the axonal projections arising from the posterior intralaminar thalamic nuclei in the rat. *Eur J Neurosci* 8: 329–343, 1996.

Desîlets-Roy B, Varga C, Lavallée P, Deschênes M. Substrate for cross-talk inhibition between thalamic barreloids. *J Neurosci* 22: RC218, 2002.

Graybiel AM, Elde RP Somatostatin-like immunoreactivity characterizes neurons of the nucleus reticularis thalami in the cat and monkey. *Journal of Neuroscience* 3: 1308–1321, 1983.

Halassa MM, Chen Z, Wimmer RD, Brunetti PM, Zhao S, Zikopoulos B, Wang F, Brown EN, Wilson MA. State-dependent architecture of thalamic reticular subnetworks. *Cell* 158: 808–821, 2014.

Oertel WH, Graybiel AM, Mugnaini E, Elde RP, Schmechel DE, Kopin IJ. Coexistence of glutamic acid decarboxylase- and somatostatin-like immunoreactivity in neurons of the feline nucleus reticularis thalami. *Journal of Neuroscience* 3: 1322–1332, 1983.

Paz JT, Davidson TJ, Frechette ES, Delord B, Parada I, Peng K, Deisseroth K, Huguenard JR. Closed-loop optogenetic control of thalamus as a tool for interrupting seizures after cortical injury. *Nat Neurosci* 16: 64–70, 2013.

Pinault D, Deschênes M. Anatomical evidence for a mechanism of lateral inhibition in the rat thalamus. *Eur J Neurosci* 10: 3462–3469, 1998a.

Pinault D, Deschênes M. Projection and innervation patterns of individual thalamic reticular axons in the thalamus of the adult rat: a three-dimensional, graphic, and morphometric analysis. *J Comp Neurol* 391: 180–203, 1998b.

Sun Q-Q, Huguenard JR, Prince DA. Somatostatin inhibits thalamic network oscillations in vitro: actions on the GABAergic neurons of the reticular nucleus. *J Neurosci* 22: 5374–5386, 2002.